Chem Soc Rev

TUTORIAL REVIEW

View Article Online
View Journal | View Issue

Cite this: *Chem. Soc. Rev.*, 2024, **53**, 5366

Platinum complexes with aggregation-induced emission†

Sheng-Yi Yang,‡[a] Yingying Chen,‡[a] Ryan T. K. Kwok,*[a] Jacky W. Y. Lam*[a] and Ben Zhong Tang *[ab]

Transition metal-containing materials with aggregation-induced emission (AIE) have brought new opportunities for the development of biological probes, optoelectronic materials, stimuli-responsive materials, sensors, and detectors. Coordination compounds containing the platinum metal have emerged as a promising option for constructing effective AIE platinum complexes. In this review, we classified AIE platinum complexes based on the number of ligands. We focused on the development and performance of AIE platinum complexes with different numbers of ligands and discussed the impact of platinum ion coordination and ligand structure variation on the optoelectronic properties. Furthermore, this review analyzes and summarizes the influence of molecular geometries, stacking models, and aggregation environments on the optoelectronic performance of these complexes. We provided a comprehensive overview of the AIE mechanisms exhibited by various AIE platinum complexes. Based on the unique properties of AIE platinum complexes with different numbers of ligands, we systematically summarized their applications in electronics, biological fields, *etc.* Finally, we illustrated the challenges and opportunities for future research on AIE platinum complexes, aiming at giving a comprehensive summary and outlook on the latest developments of functional AIE platinum complexes and also encouraging more researchers to contribute to this promising field.

Received 6th March 2024

DOI: 10.1039/d4cs00218k

rsc.li/chem-soc-rev

Key learning points

1. The design strategies and applications of AIE cyclometallic platinum complexes.
2. The effects of the molecular structure, coordination mode, and aggregation environment of AIE cyclometallic platinum complexes.
3. The AIE mechanisms of cyclometallic platinum complexes.
4. The challenges for AIE cyclometallic platinum complexes and the prospects for their future development were discussed.

1. Introduction

Aggregation-induced emission (AIE) is a phenomenon in which certain molecules exhibit low or no fluorescence efficiency when present as monomers, but their fluorescence properties are significantly enhanced when the molecules aggregate to form aggregates. This phenomenon is opposite to that of conventional fluorescent molecules, which emit light in solution but undergo quenching in the aggregated state or at high concentrations, known as the phenomenon of aggregation-caused quenching (ACQ).[1] Since the introduction of the concept of AIE by Tang *et al.* in 2001, rapid development of AIE-functionalized compounds has been observed.[2–5] Among them, AIE metal complexes represent an important subgroup of the AIE family.[2,6–8] For example, in 2002, Lu *et al.* reported the AIE phenomenon of rhenium complexes, initiating a new era for AIE phosphorescent complexes.[9] In the same year, Yam *et al.* reported the self-assembly behavior of tridentate cyclometalated platinum(II) complexes and discovered the luminescence enhancement of these complexes in the aggregate state attributed to the Pt–Pt interactions.[10] Compared to AIE iridium (Ir),[11] rhenium (Re),[12] gold (Au),[13] zinc (Zn),[14] and copper (Cu) complexes,[15] AIE platinum complexes exhibit significant

[a] *Hong Kong Branch of Chinese National Engineering Research Center for Tissue Restoration and Reconstruction, Division of Life Science, State Key Laboratory of Molecular Neuroscience, and Department of Chemical and Biological Engineering, The Hong Kong University of Science and Technology, Clear Water Bay, Kowloon, Hong Kong 999077, China. E-mail: chryan@ust.hk, chjacky@ust.hk*
[b] *School of Science and Engineering, Shenzhen Institute of Aggregate Science and Technology, The Chinese University of Hong Kong, Shenzhen (CUHK-Shenzhen), Guangdong 518172, China. E-mail: tangbenz@cuhk.edu.cn*

† Electronic supplementary information (ESI) available. See DOI: https://doi.org/10.1039/d4cs00218k

‡ These authors contribute equally.

variations in their optoelectronic properties due to the differences in their ligand number, ligand structure, oxidation state, coordination mode, geometric shape, stacking state, and aggregation environment (Table S1, ESI†). These variations provide AIE platinum complexes with significant research and application value.[2,6–8]

AIE platinum complexes reveal diverse optoelectronic properties and hold great promise for various applications on account of their versatile coordination modes and molecular structures. However, existing reviews on AIE platinum complexes suffer from certain limitations.[6–8] First, only a small fraction of AIE platinum complexes are covered, lacking a comprehensive and systematic discussion. Second, recent advancements in the development of novel AIE platinum complexes and the exploration of new AIE mechanisms and their applications require a corresponding review to summarize and discuss this progress. Last, a comprehensive analysis is lacking for the relationship between molecular structures, properties, and applications in previous reviews.[2,6–8]

In this review, based on the number of ligands in platinum complexes, mononuclear platinum complexes are classified into five categories. Among them, platinum complexes with a two-ligand framework were further divided into homoleptic bidentate ligand, heteroleptic bidentate ligand, and tridentate ligand complexes (Fig. 1A). Furthermore, based on the types of bridging groups in polynuclear platinum complexes, they are classified into three categories (Fig. 1B). In Fig. 1C, the development history of AIE platinum complexes is detailed according to the number of ligands, and the corresponding molecular structures as well as their AIE mechanisms are provided for better understanding. So far, there have been approximately ten proposed AIE mechanisms based on cyclometalated platinum complexes, including restriction of intramolecular motion (RIM),[5–8,16–19] Pt–Pt interactions,[10,20–23] restricted distortion of excited-state structure (RDES),[24,25] restriction of coordination skeletal deformation (RCSD),[26–28] restrained D_{2d} deformation of the coordinating skeleton,[29] restriction of molecular configuration transformation (RMCT),[30] dimer emission,[31] and

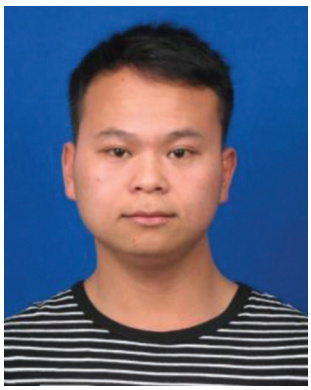

Sheng-Yi Yang

Sheng-Yi Yang received his MS degree from Xiangtan University under the guidance of Prof. Weiguo Zhu in 2018. He received his PhD in 2022 from Soochow University under the guidance of Prof. Zuo-Quan Jiang and Prof. Liang-Sheng Liao. Currently, he is conducting postdoctoral research in Prof. Ben Zhong Tang' group at The Hong Kong University of Science and Technology (HKUST). His research interests are mainly focused on the design and synthesis of organic optoelectronic materials in chiral chemistry, photophysical chemistry, and their organic light-emitting diode and biological applications.

Yingying Chen

Yingying Chen received her MS degree from Xinan University under the supervision of Prof. Cheng-He Zhou in 2018. She received her PhD in 2022 from Wuhan University under the supervision of Prof. Fuan Wang. She is now carrying out her postdoctoral research in Prof. Ben Zhong Tang' group at HKUST. Her research interests are mainly in the development of functional nucleic acid nanomaterials, DNA-AIE composite probes, and the exploration of their biological applications in early diagnosis and treatment of tumors.

Ryan T. K. Kwok

Ryan T. K. Kwok received his PhD degree from HKUST in 2013 under the supervision of Prof. Ben Zhong Tang. He worked as a Research Associate in Professor Ben Zhong Tang's research group from 2013 to 2017. His research focuses on the development of functional AIE materials and exploration of their applications in biological imaging and sensing.

Jacky W. Y. Lam

Jacky W. Y. Lam received his PhD degree from HKUST in 2003 under the supervision of Prof. Ben Zhong Tang. In 2003–2007, he carried out his postdoctoral work on novel polymers with linear and hyperbranched structures and advanced functional properties in the Tang group. He is currently a research associate professor in the Department of Chemistry at HKUST.

the oxygen-shielding effect.[32] These mechanisms will be further explained in the subsequent section. Based on the unique properties of AIE platinum complexes with different numbers of ligands, we systematically introduce their applications. For instance, platinum(II) complexes,[18] and polynuclear platinum complexes[19] with two-ligand,[33–36] three-ligand molecular frameworks, rigid molecular structures and high quantum yields are suitable for optoelectronic devices.[37] Platinum(II) complexes with four-ligand molecular frameworks and platinum(IV) complexes with six-ligand molecular frameworks, on the other hand, have found extensive applications in the field of biomedical imaging and therapy due to their correlation with cisplatin drugs.[38–41] Platinum(II) complexes with two-ligand molecular frameworks and tridentate ligands, owing to their significant Pt–Pt interactions and pronounced multi-stimuli response under external stimuli, have found broad applications in detection and sensing.[20,21,42,43] This review explores interdisciplinary ideas and can serve as a valuable learning resource for researchers in this field.

2. Platinum complexes with aggregation-induced emission

2.1 One-ligand molecular framework

Platinum(II) complexes with one-ligand molecular frameworks refer to cyclometalated platinum(II) complexes that contain only one ligand. These complexes are also known as tetradentate ligand complexes. Based on the ligand structure, they can be roughly classified into porphyrin-,[44] Schiff base-,[45] polypyridine-,[46] N-heterocyclic carbene-,[47] and phthalocyanine-cyclometalated platinum(II) complexes.[48] Taking into account the structural elements that impact the efficiency, chromatic purity, and durability of luminescence, incorporating rigid tetradentate ligand frameworks comprising robust σ-donating atoms proves advantageous in the quest to engineer exceptionally stable cyclometalated platinum(II) complexes. For example, expanding the π-conjugated system of porphyrin-/phthalocyanine-cyclometalated platinum(II) complexes (**Pt1**, **Pt2**) is an effective method to achieve near-infrared (NIR) absorption and phosphorescence.[48–50] However, these classical four-coordinate complexes tend to exhibit an aggregation-caused quenching effect due to their planar square geometry (Fig. 2A). To weaken the ACQ effect of molecules, on the one hand, large steric hindrance groups are introduced on the planar skeleton of the molecules to weaken the π–π stacking (**Pt3**).[50] On the other hand, a twisted polycyclic aromatic hydrocarbon skeleton is constructed to break the planar molecular structure, thereby affecting the stacking method, and realizing the transformation of molecules from the ACQ to AIE effect.[51]

Up to now, the AIE properties of Schiff base platinum complexes have been widely reported.[45,52,53] In 2004, Che *et al.* reported a Schiff base-based cyclometalated platinum(II) complex (**Pt4**) with strong phosphorescence both in acetonitrile solution and solid state at room temperature.[52] As shown in Fig. 2B, the π–π stacking of the molecule was effectively suppressed due to the steric hindrance of the four methyl groups on the ligand. Additionally, numerous C–H···π interactions between molecules were present, which effectively suppressed non-radiative transitions. To further increase the steric hindrance, in 2011, Naota *et al.* reported a series of arched platinum(II) complexes with *trans*-bis(salicylaldehyde diamine) and different lengths of alkyl or alkoxyl linkers (**Pt5**, **Pt6**, and **Pt8**).[22] By changing the type of bridging group, the stacking method between molecules is adjusted. Compared to **Pt5**, due to the Pt–Pt interactions, the photoluminescence quantum yield (PLQY) of **Pt6** (crystal state, room temperature) is significantly improved to 32.0%. Furthermore, **Pt8** with a polyethylene glycol bridge exhibited strong yellow phosphorescence at 298 K. The PLQY of the crystal at 298 K was determined to be 38.0%, which was the highest value for phosphorescent crystal emission at that time. At room temperature, **Pt8** exhibited almost no emission in different polar solvents (cyclohexane, PLQY < 0.1%; 2-methyl tetrahydrofuran, PLQY < 0.1%), and the amorphous solid of **Pt8** showed a lower PLQY (14.0%, room temperature), indicating that crystal packing minimized the energy loss of phosphorescence. Single-crystal structure analysis revealed that **Pt8** formed molecular dimers through intermolecular Pt–Pt interactions, and there existed a hydrogen bonding network between adjacent polyethylene glycol units. These intermolecular interactions in the crystal hindered non-radiative transition pathways, resulting in crystallization-induced emission.

In 2019, Naota *et al.* further developed a series of arched *trans*-bis[2-(aminomethyl)imidazolyl] platinum(II) complexes with multiple methylene linkers and found that this complex did not exhibit the ACQ phenomenon over the entire concentration range.[31] Take **Pt9** as an example, based on the single-crystal structure analysis (Fig. 2B), the AIE phenomenon of **Pt9** was attributed to the increased contribution of metal–metal–

Ben Zhong Tang

Ben Zhong Tang received his PhD degree from Kyoto University, Japan, in 1988. He conducted his postdoctoral work at the University of Toronto, Canada, in 1989–1994. He joined HKUST in 1994 and was promoted to a chair professor in 2008 and the Stephen K. C. Cheong Professor of Science in 2013. He was elected to the Chinese Academy of Sciences in 2009. In 2021, he joined Chinese University of Hong Kong, Shenzhen as the Dean of School of Science and Engineering, and he is now the Distinguished Presidential Chair Professor. He is now serving as an Editor-in-Chief of Aggregate. His research interests include the exploration of new AIE materials, new luminescent processes, fluorescent probes, and new polymerization reactions.

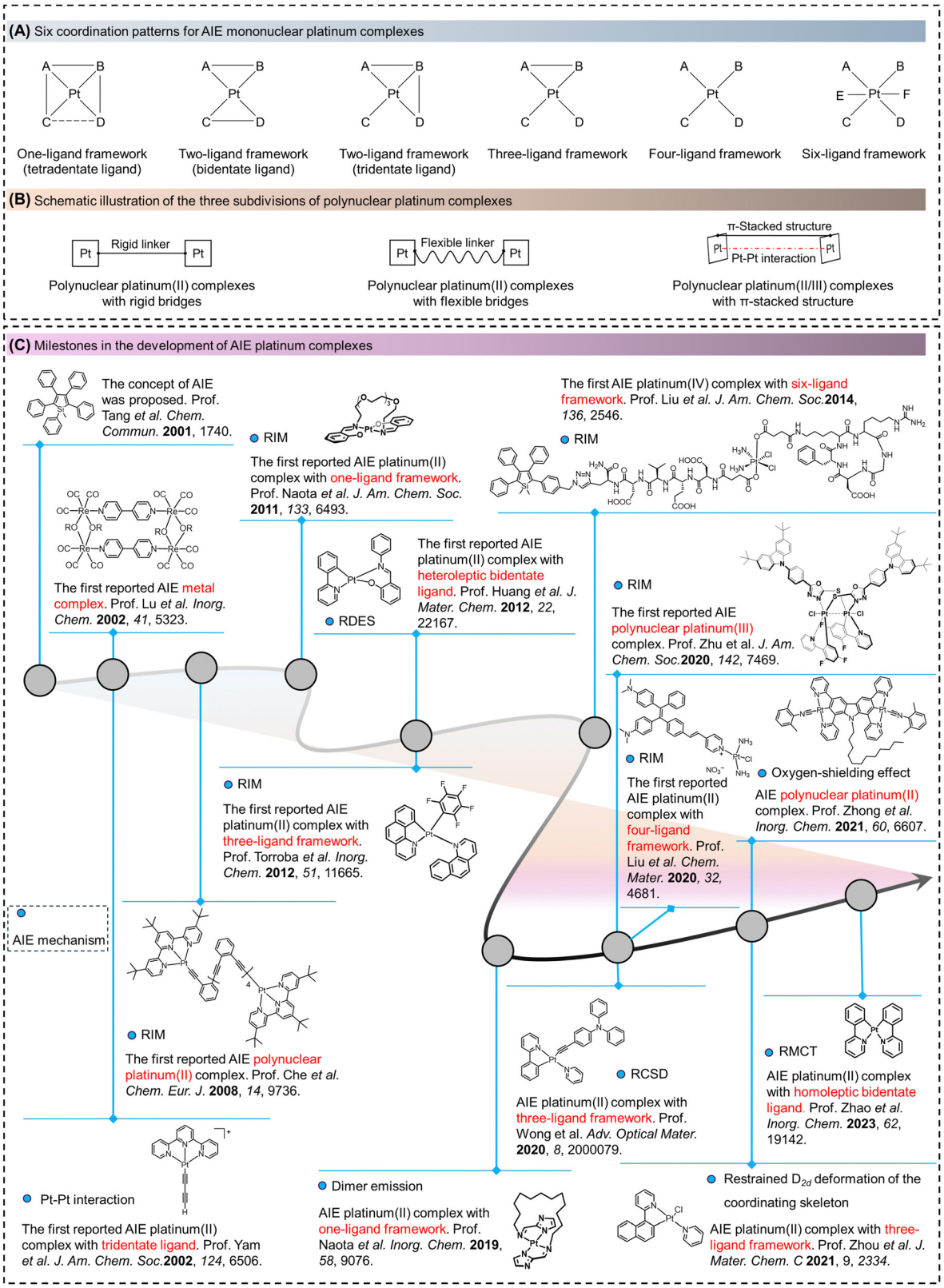

Fig. 1 (A) Six coordination patterns for AIE mononuclear platinum complexes. (B) Schematic illustration of the three subdivisions of polynuclear platinum complexes. (C) Milestones in the development of AIE platinum complexes.

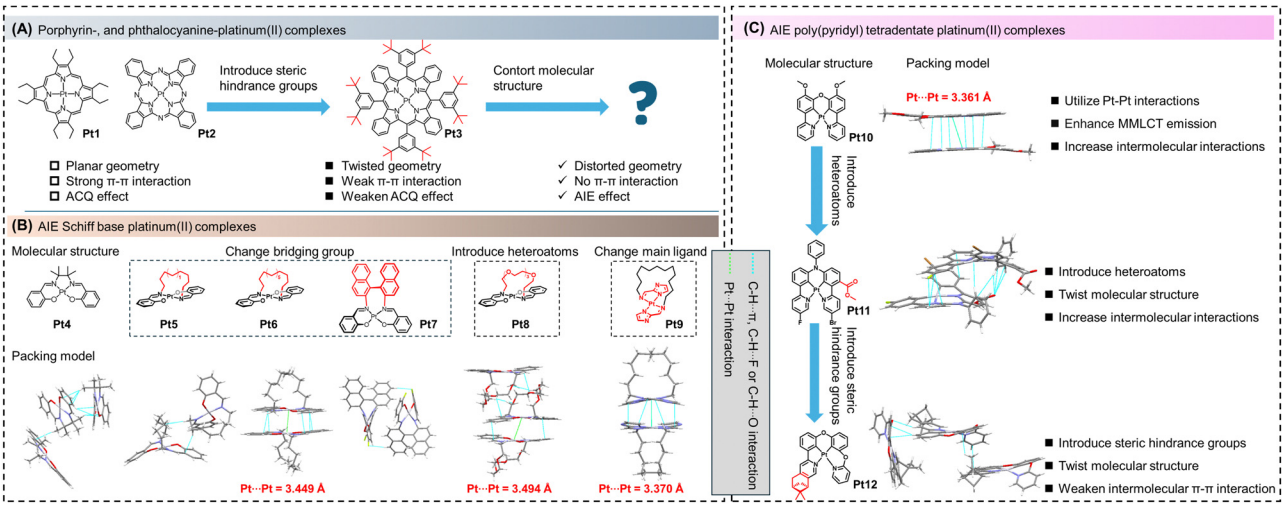

Fig. 2 AIE cyclometalated platinum(II) complexes with one-ligand molecular frameworks. Molecular structures, single crystal structures, stacking modes of cyclometalated platinum(II) complexes based on (A) porphyrin, and phthalocyanine-ligand, (B) Schiff base ligand, and (C) poly(pyridyl) tetradentate ligand.

ligand charge transfer (MMLCT) to the ground-state transition. In addition to alkyl or alkoxyl chains as linking groups, in 2018, Xiang *et al.* reported a Schiff base-cyclometalated platinum(II) complex (**Pt7**) with larger steric hindrance introduced by 1,1′-binaphthyl linkers. Due to the restricted movement of the central 1,1′-binaphthyl moiety, **Pt7** exhibited unusual near-infrared aggregation-induced phosphorescence in a THF/H_2O mixture or solid state. Thus, by introducing functional groups with significant steric hindrance to the Schiff base framework, the π–π stacking could be effectively suppressed, which weakened the ACQ effect but promoted the AIE property achieved, following the design principles.[54]

Poly(pyridyl) tetradentate platinum(II) complexes are another class of AIE cyclometalated platinum(II) complexes with one-ligand molecular frameworks. In 2020, MacLachlan *et al.* reported a rigid oxygen-bridged bis(phenylpyridine)-containing platinum(II) complex (**Pt10**) with AIE properties. From the single-crystal structure analysis, significant Pt–Pt interactions were found to be a cause of the transformation of the long-wavelength emission into the dimeric emission (Fig. 2C).[55]

In 2022, Tunik *et al.* reported an asymmetric nitrogen-bridged bis(phenylpyridine) platinum(II) complex (**Pt11**) with AIE characteristics in a THF/H_2O mixture. According to the single-crystal structure analysis, introducing heteroatoms (F, Cl, and O atoms) into the molecular skeleton, the AIE effect originated from intermolecular interactions such as C–H···π and C–H···O, in aggregates (Fig. 2C).[56] In the same year, Zhang *et al.* reported a rigid oxygen-bridged *p*-menthane-modified tetradentate cyclometalated platinum(II) complex (**Pt12**).[16] **Pt12** exhibited significant aggregation-enhanced emission (AEE) in a DMSO/H_2O mixture (5×10^{-5} mol L^{-1}) with a high PLQY of 73.2%. Single-crystal structure analysis (Fig. 2C) revealed that the introduction of the *p*-menthane group effectively suppressed π–π stacking between **Pt12** molecules due to steric hindrance. Additionally, the incorporation of multiple C–H···π interactions played a synergistic role, leading to the observed AEE phenomenon.[16] As mentioned above, platinum(II) porphyrins, platinum(II) tetrapyrrolic macrocycles, and platinum(II) phthalocyanines have larger π–π stacking and more planar geometries, which typically show the ACQ rather than AIE effect. To overcome the ACQ phenomenon, on the one hand, we need to introduce functional groups with large spatial hindrances to prevent intermolecular π–π stacking. Furthermore, in general, the energy gap law and its inherent influence on luminescence, especially in the NIR region, need to be considered. The energy gap law is a recognized phenomenon that describes the lower emission intensities observed in the NIR region for polyatomic molecules in the condensed phase. According to this law, the main mechanism responsible for the quenching of NIR emission is non-radiative deactivation, which occurs due to the energy gap between the excited state and the ground state of the molecule. On the other hand, how to utilize the planar configuration of cyclometalated platinum(II) complexes and Pt–Pt interactions to construct luminescent dimers and enhance the contribution of ^{3}MMLCT to the ground-state transition is an effective approach to addressing the ACQ phenomenon in planar cyclometalated platinum(II) complexes. Additionally, a feasible strategy is to decompose tetradentate ligands into bidentate and/or tridentate ligands to obtain platinum(II) complexes with AIE properties. Another viable strategy is to further oxidize tetradentate platinum(II) complexes to construct platinum(II/IV) complexes with π-stacking structures or binuclear platinum(II) or platinum(III) complexes, which will be discussed in subsequent sections.[19,38,41]

2.2 Two-ligand molecular framework

2.2.1 Homoleptic bidentate ligand platinum(II) complexes. Homoleptic bidentate ligand platinum(II) complexes can be derived from tetradentate ligand platinum(II) complexes, for

example, breaking the porphyrin-like structure and anchoring it with a platinum ion. Homoleptic bidentate platinum(II) complexes acquire rich modification sites, enabling the multi-functional derivatization of these platinum(II) complexes. Moreover, these homoleptic bidentate cyclometalated platinum(II) complexes exhibit excellent molecular rigidity and self-assembly properties, leading to their rapid development in recent years.[30,33–36,57,58]

In 2017, Chi *et al.* designed and synthesized a novel bipyrazole cyclometalated platinum(II) complex (**Pt13**, Fig. 3A).[34] The presence of multiple nitrogen atoms in the complex reduced the electron density around the metal centre. The introduction of trifluoromethyl groups further enhanced the electron-deficiency of the complex. Additionally, the incorporation of less sterically hindered trifluoromethyl groups facilitates the formation of crystalline thin films. Grazing angle X-ray diffraction analysis revealed that **Pt13** exhibited a tilted domino-like stacking arrangement, with Pt–Pt distances of around 3.9–4.2 Å and intermolecular π–π distances of 3.4–3.7 Å. As a result, **Pt13** displayed steady-state absorption spectra in a thin film state, indicative of MMLCT transitions.[33,34]

To further shift the MMLCT emission to longer wavelengths, in 2020, Chi *et al.* replaced the bipyrazole ligand with a pyridine ligand containing a pyrimidine group and constructed a homoleptic bidentate cyclometalated platinum(II) complex abbreviated as **Pt14**. Compared to **Pt13**, **Pt14** with solid-state exhibited further red-shifted emission at 866 nm and a PLQY of 12%.[35] In 2022, the research group further expanded the conjugation degree of the ligands and developed **Pt15**, which emitted light at 965 nm with a high PLQY of 13.3% (vacuum deposited thin film, room temperature).[36] Although the AIE properties of these molecules were not tested, a detailed analysis revealed that these complexes utilized intermolecular Pt–Pt interactions and π–π interactions to adopt a domino-like stacking arrangement and MMLCT to induce NIR emission.[33]

This class of molecules showing AIE behaviors was characterized and reported in 2020. Carlos *et al.* prepared a bidentate AIE-active cyclometalated platinum(II) complex with a homoleptic bidentate ligand (**Pt16**).[57] Due to the hydrogen bonding between the two coordinating ligands, these complexes maintained planarity similar to that of tetradentate ligand platinum(II) complexes. By introducing alkoxyl chains to the ligands, these complexes further revealed liquid crystalline properties. They could self-assemble into nanoparticles through intermolecular Pt–Pt interactions induced by Hg^{2+} and displayed AIE properties.

As mentioned above, up to now, achieving control over the AIE properties requires striking a balance between the strength of π–π/Pt–Pt interactions and the steric hindrance between complexes.[57] It was deduced that by introducing appropriate heteroatoms or functional groups to ligands, the molecular structure can be modulated to alter the aggregation mode. On the other hand, by introducing heteroatoms or functional

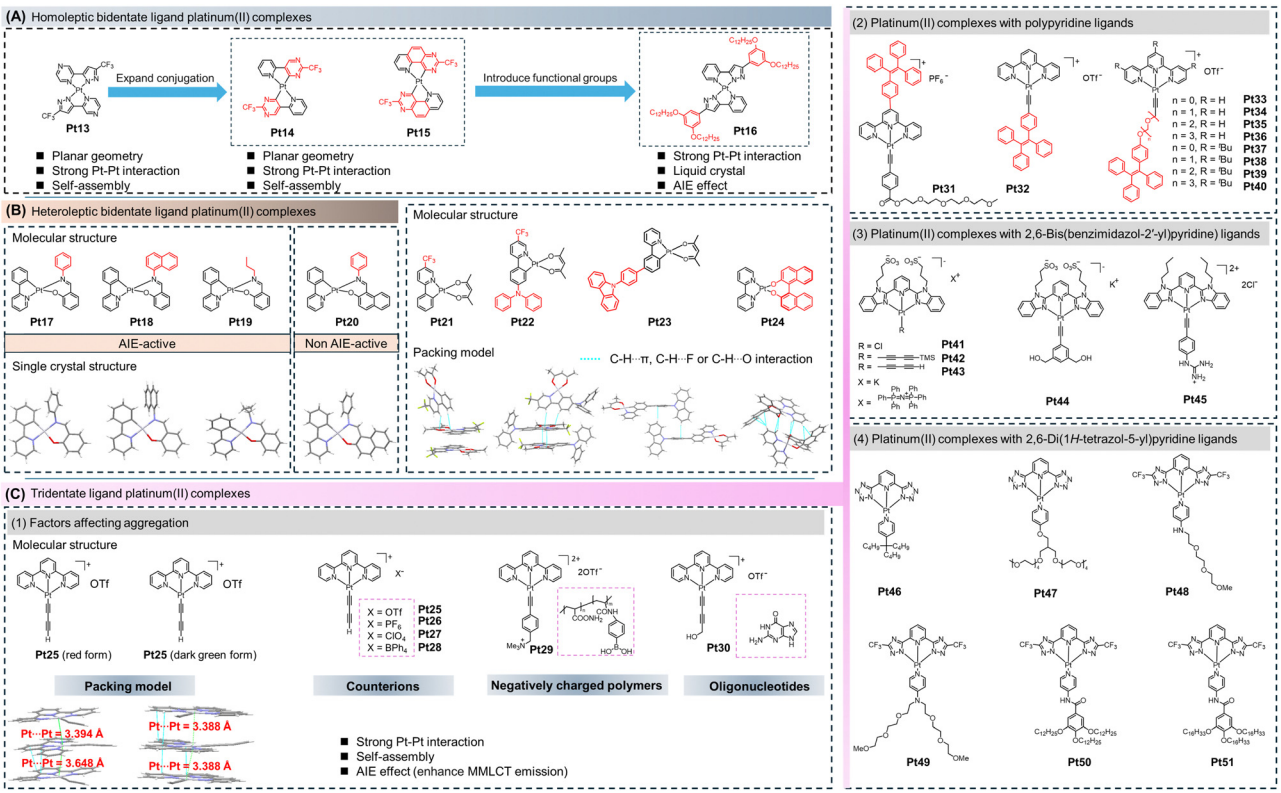

Fig. 3 AIE cyclometalated platinum(II) complexes with two-ligand molecular frameworks. Molecular structures, single crystal structures, stacking modes of cyclometalated platinum(II) complexes based on (A) homoleptic bidentate ligands, (B) heteroleptic bidentate ligands, and (C) tridentate ligands.

groups, the photophysical properties of the complexes can be modified to meet the requirements of different applications.[58]

2.2.2 Heteroleptic bidentate ligand platinum(II) complexes. Heteroleptic bidentate cyclometalated platinum(II) complexes refer to cyclometalated platinum(II) complexes with two different bidentate ligands. Compared to bidentate homoleptic cyclometalated platinum(II) complexes, these complexes possess greater flexibility and variety in molecular structure and types.[6–8,17,24,25] By introducing different functional groups into the ligands, the derivatization options, the number of complexes, and the applications can be notably increased.[59,60] Until now, many bidentate heteroleptic complexes with AIE properties have been reported. According to the type of ligands, the most classic complexes include phenyl-pyridine complexes and Schiff base complexes (Fig. 3B).

In 2012, Huang *et al.* reported a series of heteroleptic bidentate platinum(II) complexes (**Pt17**–**Pt20**).[24] Among them, **Pt17**, **Pt18**, and **Pt19** are AIE-active while **Pt20** does not display the AIE phenomenon. **Pt17** showed a high PLQY of 38.0% (crystal state) at room temperature. In **Pt17**, **Pt18**, and **Pt19**, the phenyl, naphthyl and alkyl chain groups could act as rotors to consume the excited-state energy through nonradiative relaxation pathways. Thus, their AIE behaviours could be explained by the RIM mechanism. However, for **Pt20**, there was an obvious rotor in the molecular structure, yet it did not exhibit distinct AIE properties. Therefore, the RIM mechanism may not be the sole origin of the AIE properties in these cyclometalated platinum(II) complexes. Experimental and theoretical calculations uncovered that in the crystalline state of **Pt17**–**Pt19**, the structural deformations from the ground state to the excited state were restricted, allowing the complexes to maintain their geometric shape upon excitation. As a result, the RDES involving the phenyl-pyridine ligands contributed to the efficient emission in the crystalline state (Fig. 3B).[24,25]

The AIE properties of molecules can be availably modulated by changing the ligand structure, which affects the molecular packing and excited-state geometry. In line with this strategy, in 2021, Liu *et al.* explored the AIE properties of cyclometalated platinum(II) complexes (**Pt21**, **Pt22**) with phenyl pyridine derivatives as the main ligands and acetylacetone as the ancillary ligand (Fig. 3B).[17] The results showed that **Pt21** exhibited ACQ behavior in a dichloromethane/*n*-hexane system. For **Pt21**, as the content of *n*-hexane increased in the solution, the emission intensity gradually decreased but maintained a certain level while **Pt22** exhibited AIE properties. The single-crystal structures showed that **Pt21** had a planar configuration without Pt–Pt interactions but had a significant number of C–H$\cdots\pi$, C–H$\cdots$F, and C–H$\cdots$O interactions. Hence, it retained emission intensity in the aggregated state. In the case of **Pt22**, the introduction of a diphenylamine group acted as a rotor. Initially, its emission intensity in dichloromethane was lower than that of **Pt21**. However, numerous intermolecular interactions in the aggregated state restricted molecular motion, resulting in the classical AIE phenomenon. Similarly, Yang *et al.* further modified the phenyl-pyridine ligand and constructed an AIE-active cyclometalated platinum(II) complex (**Pt23**), as shown in Fig. 3B.[60] This series of work demonstrated that introducing bulky functional groups on the planar phenyl-pyridine ligands efficiently modulated the molecular packing. By utilizing intermolecular interactions, nonradiative transitions were effectually suppressed, resulting in the AIE properties of the complexes.

Based on these results, introducing bulky functional groups on rigid ligands and influencing the molecular arrangement and various intermolecular interactions, such as Pt–Pt interactions, C–H$\cdots\pi$, or π–π interactions, can affect the phosphorescence properties of the complexes in the solid-state. In 2023, Nishikawa *et al.* utilized the binaphthol group and bipyridine group to construct a cyclometalated platinum(II) complex, **Pt24**.[59] As shown in Fig. 3B, due to the direct coordination of the binaphthol with the platinum(II) ion, a twisted seven-membered ring structure was formed. This twisted structure caused weak emission in the solution state. However, in the solid state, molecular motion was restricted, and the twisted structure suppressed π–π interactions between the molecules. The intermolecular interactions in **Pt24** effectively suppressed nonradiative transitions, resulting in pronounced AIE properties in the solid-state or THF/H_2O system.[59]

2.2.3 Tridentate ligand platinum(II) complexes. Platinum(II) complexes with pyridine-related tridentate ligands, such as bipyridine or terpyridine, exhibit rich photophysical properties. These complexes typically exhibit polymorphism, with wide absorption and emission ranges in the solid state. The Pt–Pt and π–π interactions between the tridentate cyclometalated platinum(II) complexes are recognized to be the source of molecular polymorphism, owing to the square planar coordination geometry of the platinum(II) ion (Fig. 3C).[10,61–63]

In 2002, Yam *et al.* reported a cyclometalated platinum(II) complex with a tridentate ligand (**Pt25**) based on a terpyridine ligand and a butadiynyl ligand.[10] Recrystallization of **Pt25** yielded two different crystal forms: one was red (from evaporation of an acetone solution), and the other was deep green (from an ether/acetonitrile system). Crystal analysis clarified that in the deep green crystal form, the complexes were evenly spaced, with a Pt–Pt distance of 3.388 Å. In the red crystal form, the complexes exhibited a zig-zag arrangement with different Pt–Pt distances of 3.394 Å and 3.648 Å, respectively. Changes in the molecular arrangement and the degree of Pt–Pt and π–π interactions result in crystals of different colors (Fig. 3C). A series of studies reported by Yam *et al.* showed that the absorbance and emission wavelengths in these solvent-induced self-assembled structures are influenced by the nature of the counterions (**Pt25**–**Pt28**),[61] negatively charged polymers (**Pt29**),[62] and oligonucleotides (**Pt30**).[63] The driving force behind the self-assembly is the electrostatic binding between the complexes and polymers, bringing the complexes closer to each other and triggering Pt–Pt and π–π interactions, resulting in significant color changes and enhanced emission.

To date, these platinum complexes have been roughly divided into three categories based on the ligand type, namely cyclometalated platinum(II) complexes with polypyridine ligands,[64,65] 2,6-bis(benzimidazol-2′-yl)pyridine ligands,[43,66,67]

and 2,6-di(1*H*-tetrazol-5-yl)pyridine ligands (Fig. 3C).[68–71] In 2017, Yam *et al.* reported a series of tridentate cyclometalated platinum(II) complexes (**Pt32**–**Pt40**, Fig. 3C) with tetraphenylethene-modified alkyne ligands. The introduction of tetraphenyl ethene groups resulted in AIE properties, and self-assembly formed stable MMLCT behavior driven by Pt–Pt and/or π–π interactions.[64] By introducing different lengths of hydrophilic groups on the terpyridine ligand to modulate its hydrophilicity, **Pt32**–**Pt36** successfully formed different self-assembled supramolecular structures (including nanorods, nanospheres, nanowires, and nanosheets) in an acetonitrile/H_2O system. It elucidates that the introduction of alkyl ether chains does not hinder aggregation. In contrast, when *t*-butyl groups were introduced into the molecule, the lower energy absorption of **Pt40** exhibited a linear relationship with the water content at 90%, expounding the absence of Pt–Pt interactions during the aggregation process, which implied that the introduction of *t*-butyl could effectively restrict the intermolecular Pt–Pt interactions. Interestingly, in 2018, Wong *et al.* incorporated tetraphenylethene groups on the terpyridine ligand rather than on the alkynyl ligand, and constructed an AIE tridentate cyclometalated platinum(II) complex (**Pt31**, Fig. 3C).[65] Owing to the tendency of **Pt31** to form molecular aggregates in water, in an acetonitrile/H_2O mixtures, a NIR emission peak at 730 nm was observed when the water content reached 70%. This emission peak can be attributed to the MMLCT emission induced by solvent-promoted Pt–Pt and/or π–π interactions in the aggregated state. By comparing the work of Yam and Wong *et al.*, the introduction of a molecular rotor into a rigid terpyridine-based platinum(II) complex can validly impart the AIE properties to the molecule without affecting the Pt–Pt interaction of the molecule. At the same time, we need to note that this type of platinum(II) complex may contain multiple AIE mechanisms, such as RIM and Pt–Pt interactions, which will be explained in subsequent sections.

In 2011, Yam *et al.* reported a series of water-soluble tridentate cyclometalated platinum(II) complexes containing hydrophilic anionic benzimidazole ligands (**Pt41**–**Pt43**). Interestingly, **Pt41** (with K^+ as the cation) disclosed a strong solvent-induced color changing phenomenon in an acetone/H_2O mixture. The prevailing notion suggests that creating a more hydrophobic environment would promote the aggregation of sulfonate ionic heads, thereby facilitating the formation of nanofibers or nanorods through enhanced Pt–Pt and π–π interactions.[66] In 2017, Yam *et al.* further designed and synthesized a water-soluble anionic alkynyl cyclometalated platinum(II) complex (**Pt44**, Fig. 3C) with a 2,6-bis(benzimidazol-2′-yl)pyridine ligand.[42] It was found that **Pt44** underwent supramolecular self-assembly with cationic peptides rich in arginine, resulting in aggregation through intermolecular Pt–Pt and π–π interactions, and enhanced luminescence. Upon addition of pancreatic trypsin, the peptide rich in arginine undergoes hydrolysis, leading to the disassembly of **Pt44** and an obvious decrease in luminescence intensity. Therefore, this method allows for the highly sensitive screening of pancreatic trypsin inhibitors and the accurate detection of pancreatic trypsin in serum solutions. In 2021, Yam *et al.* further joined a guanidine group to construct a tridentate cyclometalated platinum(II) complex (**Pt45**).[67] The non-covalent interaction between the guanidine group and RNA induces aggregation of **Pt45**, resulting in significant emission enhancement upon binding to RNA. The authors further found that **Pt45** not only displayed pronounced spectral changes and emission enhancement upon binding to RNA but also enabled specific nucleolus imaging in cells. Compared to fluorescent dyes, **Pt45** showed red emission and a large Stokes shift, providing a high signal-to-background autofluorescence ratio for nucleolus imaging.[67]

In 2011, Cola *et al.* reported the cyclometalated platinum(II) complex **Pt46** based on the 2,6-bis(tetrazolyl)pyridine ligand.[68] By coordinating alkylpyridine auxiliary ligands to the 2,6-bis(tetrazolyl)pyridine complex, the solubility and processability of the complex were improved. **Pt46** did not emit light in dilute solution at room temperature but produced enhanced emission in frozen dichloromethane at 77 K or in thin films. The PLQY of **Pt46** in a neat film and a poly(methyl methacrylate) (PMMA) matrix reached 87%. After that, Cola *et al.* further adjusted the molecular structure by attaching two tetraethylene glycol chains to the auxiliary ligand, obtaining **Pt47** with water solubility.[69] **Pt47** formed a water gel through interaction with cyclodextrin. Then, in 2016, Cola *et al.* used the spectroscopic changes induced by Pt–Pt interactions to probe the evolution of complex supramolecular processes. The introduction of hydrophilic tri-ethylene glycol side chains made the complex **Pt48** amphiphilic.[70] Additionally, **Pt48** contained imine groups capable of participating in directional hydrogen bonding, which played crucial roles in self-assembly. They tracked each assembly in the aggregate system in real time by observing the different fluorescent colors in the aggregate state.

In 2017, Cola *et al.* further synthesized **Pt49** and applied **Pt48** and **Pt49** to the field of electrochemiluminescence, reporting for the first time the aggregation-induced electrochemiluminescence phenomenon through intermolecular Pt–Pt and π–π interactions.[71] In 2020, Xie *et al.* further adjusted the aggregation behavior of the complexes by modulating the length of alkoxyl chains and constructed the tridentate cyclometalated platinum(II) complexes **Pt50** and **Pt51**, which exhibited fluorescent liquid crystal phases in hexagonal and rectangular columnar arrangements, respectively.[72] Through intermolecular Pt–Pt and π–π interactions, **Pt50** and **Pt51** not only displayed strong luminescence and the AIE effect at high temperatures but also demonstrated a reversible vapor-induced color change under alternate vapor exposure to dichloromethane and ethanol.

The tridentate AIE cyclometalated platinum(II) complexes with two-ligand molecular framework show rich photophysical changes at the molecular level when in the aggregated state due to their planar rigid structures. The intermolecular Pt–Pt and π–π interactions impart prominent variations in absorption and emission, which are manifested macroscopically. The luminescent properties of this series of molecules are highly dependent on factors such as temperature, type of counterions, and

solvent systems. Therefore, tridentate AIE cyclometalated platinum(II) complexes with a two-ligand molecular framework can serve as detectors for specific influencing factors.[21]

2.3 Three-ligand molecular framework

As mentioned above, the photophysical properties of platinum(II) complexes can be easily modulated by altering the ligand structure. However, conventional cyclometalated platinum(II) complexes, such as AIE platinum(II) complexes with one-ligand or two-ligand molecular frameworks, have a rigid planar structure that tends to form close π–π stacking, causing limited variations in the emission spectra. Additionally, it is relatively challenging to simultaneously introduce electron donors and acceptors into a single molecule in these two molecular systems to improve the electron and hole injection/transfer processes.[73–77] Therefore, platinum(II) complexes with a three-ligand molecular framework have emerged, where the complexes consist of one bidentate ligand and two independent monodentate ligands. This molecular structure effectively suppresses the π–π interactions observed in traditional cyclometalated platinum(II) complexes and improves the balance of electron and hole injection/transfer behavior, especially in optoelectronic devices.[28,29,73–77] Representative molecules **Pt52**–**Pt56** and their corresponding single-crystal structures are listed in Fig. 4A. For instance, in 2012, Lalinde *et al.* reported a platinum(II) complex (**Pt52**, Fig. 4A) with a three-ligand molecular framework based on phenanthroline and pentafluoro-benzene ligands.[73] **Pt52** had AIE properties in the solid state. Single-crystal structure analysis revealed that **Pt52** displayed the characteristic twisted molecular structure. From the molecular packing perspective, there were evident π–π and multi-intermolecular interactions between the pentafluorophenyl units, expounding that **Pt52** underwent aggregation-induced π–π emission in the solid state.

To construct efficient AIE platinum(II) complexes with a three-ligand molecular framework, Zhou *et al.* made significant contributions in this field.[28,29,77] In 2020, Zhou *et al.* constructed a series of cyclometalated platinum(II) complexes with a three-ligand molecular framework, **Pt57**–**Pt59**, using phenylpyridine as the main ligand, pyridine-derived groups as the second ligand, and phenyl ethynyl derivatives as the third ligand (Fig. 4B).[77] The authors systematically studied the influence of the alkynyl ligand's structure and electronic effects on the luminescent properties of the entire complexes. Compared to traditional rigid platinum(II) complexes with two bidentate ligands or one tridentate/tetradentate ligand, **Pt57**–**Pt59** have more deformation space in their planar square geometry in the ground state, allowing for a transition to a quasi-tetrahedral configuration in the excited state, resulting in poor solution emission. However, **Pt57**–**Pt59** disclosed notable AIE effects in doped films and aggregated states and possessed higher PLQY (56%, 80%, 65%, respectively) in the doped film (PMMA film doped with ≈1.0 wt% platinum complex at room temperature). This work demonstrated that restricted structural distortion

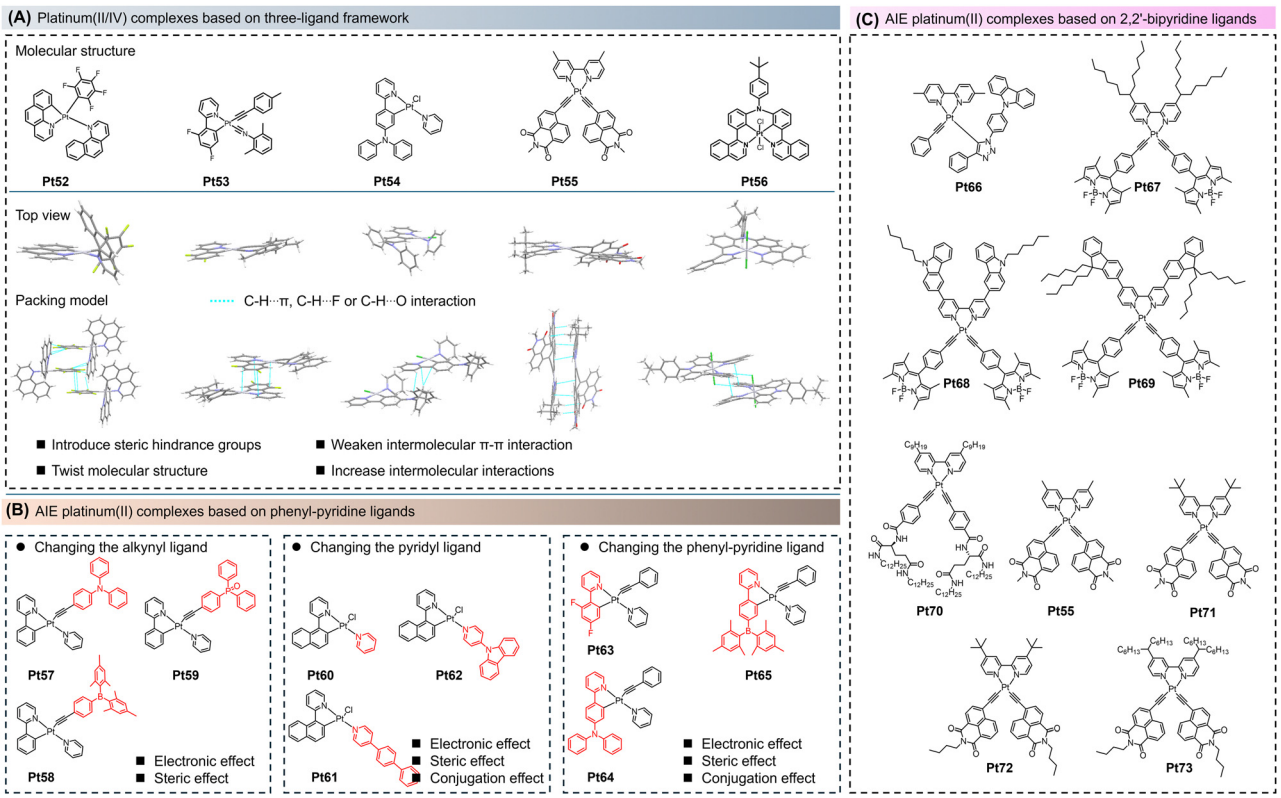

Fig. 4 (A) Overview of the molecular structures, single crystal structures, and stacking modes of platinum complexes with three-ligand molecular frameworks. (B) AIE platinum(II) complexes based on phenyl-pyridine ligands. (C) AIE platinum(II) complexes based on 2,2′-bipyridine ligands.

was one of the important mechanisms behind the AIE properties.

After that, in 2021, Zhou *et al.* replaced the phenyl-pyridine ligand with naphthyl-pyridine ligands and synthesized cyclometalated platinum(II) complexes (**Pt60–Pt62**, Fig. 4B) with a three-ligand molecular framework.[29] **Pt60–Pt62** exhibited distinct AIE effects in the THF/H_2O system. This work further investigated the influence of the pyridine-based ligand's structure and electronic properties on the luminescent performance of the entire complexes. It was found that increasing the conjugation degree of the ligands and introducing donor/acceptor structures effectively red-shifted the absorption and emission of the molecules. By extending the conjugation degree of the pyridine-based ligand, a new AIE mechanism was revealed, where the restricted structural distortion from the ground state to the excited state was the main mechanism behind the AIE properties.

Very recently, in 2023, Zhou *et al.* further systematically analyzed the impact of phenyl-pyridine ligands' structural variations on the luminescent properties of the complexes. They designed and synthesized cyclometalated platinum(II) complexes (**Pt63–Pt65**, Fig. 4B) with a three-ligand molecular framework.[28] It was revealed that introducing ligands with donor/acceptor structures could effectively regulate the electron/hole transport ability of the molecules, making them more suitable for applications in optoelectronic devices. Additionally, as mentioned earlier, the steric hindrance effect of the ligands had a significant impact on intermolecular stacking, efficiently reducing π–π stacking between molecules and suppressing the ACQ phenomenon. Thus, **Pt63–Pt65** produced substantial AIE effects in the THF/H_2O mixture.

Apart from AIE cyclometalated platinum(II) complexes with three ligands based on phenyl-pyridine ligands, rapid development was attained in AIE platinum(II) complexes with 2,2′-bipyridine ligands (**Pt55**, **Pt66–Pt73**, Fig. 4C).[75,78–80] For instance, in 2014, Yam *et al.* reported the synthesis of AIE platinum(II) complexes (**Pt66**) with a three-ligand molecular framework.[78] **Pt66** showed a low PLQY of only 18.0% in dichloromethane solution (room temperature using $[Ru(bpy)_3]Cl_2$ as a standard), but when doped in *m*CP (1,3-bis(9-carbazolyl)benzene), the PLQY increased to 71.0%, demonstrating a significant AIE effect. Additionally, **Pt66** exhibited AIE behavior in THF/H_2O mixtures. In dilute solutions, the aromatic triazole units acted as rotors and dissipated energy through non-radiative transitions, resulting in weak emission. In the aggregated state, the rigidification of **Pt66** molecules restricted their rotational motion, slowing down the non-radiative decay rate and enhancing the emission intensity of ^{3}MLCT.

In 2017, Zhu *et al.* studied a series of AIE platinum(II) complexes (**Pt67–Pt69**) with a three-ligand molecular framework. All complexes exhibit $^1\pi$–π^* transitions/^{1}MLCT absorption bands and green fluorescence originates from $^1\pi$–π^*state mixed ^{1}MLCT character. These complexes exhibited obvious AIE behavior in acetonitrile/H_2O mixtures. Moreover, this work perfectly combines AIE and optical power limiting properties in one molecule.[79] In 2019, Yam *et al.* introduced a functional group derived from L-glutamine into the bis(arylalkynyl) ligands, constructing a platinum(II) complex (**Pt70**) with a three-ligand molecular framework.[80] Due to the introduction of a long alkyl chain on the 2,2′-bipyridine ligand, the molecules aggregated through hydrogen bonding, π–π, and Pt–Pt interactions and form a metal gel at room temperature. Furthermore, in 2023, Zhu *et al.* introduced alkyl chains into the alkynylpyrene imine ligands and the 2,2′-bipyridine ligands, synthesizing a series of platinum(II) complexes (**Pt55**, **Pt71–Pt73**, Fig. 4C) with a three-ligand molecular framework.[75] It was shown that the introduction of alkyl chains had no significant impact on the absorption and emission properties of these complexes in dilute solutions but affected the AIE properties in the aggregated state. For example, in a THF/ethylene glycol mixed solvent system, the shorter alkyl chain on the 2,2′-bipyridine ligand enhanced the AIE of the complexes. However, the introduction of different alkyl chains on the alkynylpyrene imine ligand did not affect their AIE properties. Single-crystal analysis revealed that the photophysical properties of these complexes in the aggregated state were influenced by the stacking pattern due to different intermolecular interactions (**Pt55**, Fig. 4A).

2.4 Four-ligand molecular framework

Platinum(II) complexes with a four-ligand molecular framework, which are platinum(II) complexes with four monodentate ligands, generally exhibit poor luminescent properties. In these complexes, due to their highly flexible molecular structure, the excited-state molecules can undergo deactivation through nonradiative relaxation pathways, including relaxation *via* the metal-centered transitions and other nonradiative processes.[41,81]

In 2020, Thomas *et al.* reported an AIE platinum(II) complex (**Pt74**) with a four-ligand molecular framework.[81] The molecular and its single-crystal structure are shown in Fig. 5A. **Pt74** possesses a classic ethynyl platinum(II) structure, with the other two coordination sites occupied by three *tert*-butyl phosphine groups. Single-crystal analysis reveals that the two fluorophenyl rings interact coplanar with the terminal rings of adjacent molecules. Due to steric hindrance from the alkyl chains, numerous intermolecular interactions prevent π–π stacking of the molecules and reduce nonradiative transitions.

Another classic platinum(II) complex with a four-ligand framework is the cisplatin-like platinum(II) complex. Cisplatin has established great importance in the treatment of various cancers in the human body.[41,82] However, on the one hand, the application and therapeutic effectiveness of cisplatin are greatly limited by drug resistance and systemic toxicity. On the other hand, the existing cisplatin drugs cannot be tracked in terms of their mechanism of action, and the integration of diagnosis and treatment cannot be achieved. Therefore, cisplatin derivatives with AIE properties have emerged (**Pt75–Pt77**).[41,83] As shown in Fig. 5A, these complexes are generally composed of a classic AIE motif and a cisplatin derivative. On the one hand, cisplatin drugs can be tracked through the fluorescence

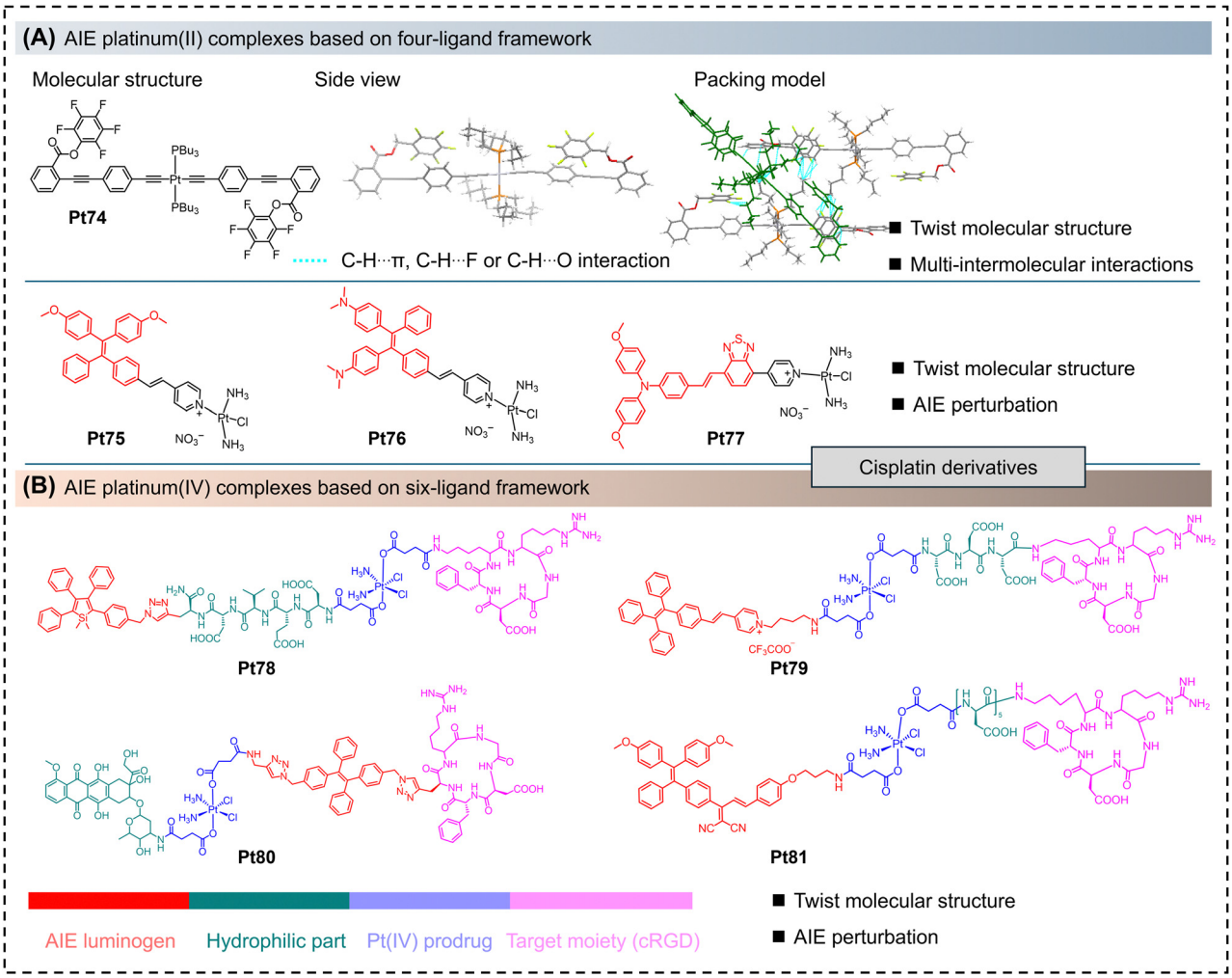

Fig. 5 (A) Molecular structures, single crystal structures, stacking modes of platinum(II) complexes with four-ligand molecular frameworks. (B) AIE platinum(IV) complexes based on the six-ligand frameworks.

imaging of AIE-active nanoparticles. On the other hand, the synergistic effect between the spin–orbit coupling of the platinum(II) center and the nanoparticles can enhance the efficiency of reactive oxygen species (ROS) generation, thereby improving the therapeutic effectiveness against tumors.

2.5 Six-ligand molecular framework

Platinum(IV) complexes with a six-ligand molecular framework are considered to be prodrugs of their platinum(II) counterparts. Octahedral platinum(IV) complexes are more resistant to ligand exchange compared to planar square platinum(II) complexes, thereby reducing adverse reactions with biomolecules before reaching the biological target and effectively lowering toxicity and side effects. Additionally, platinum(IV) complexes can easily bind to other biologically active ligands to construct multifunctional anticancer agents.[82] As shown in Fig. 5B, platinum(IV) complexes with AIE properties (**Pt78–Pt81**) have more complex molecular structures.[38–40] According to the functionalities of different molecular segments, they can be roughly divided into AIE luminophores, hydrophilic units, platinum(IV) drug precursors, and biologically active peptide chains (targeting units). Similar to the AIE unit in platinum(II) complexes with a four-ligand molecular framework, the AIE luminophore in the molecule can effectively track cisplatin drugs through fluorescence imaging. The specific details of this process will be elaborated on in the application section.

2.6 Polynuclear platinum small molecules

2.6.1 Polynuclear platinum(II) small molecules. In polynuclear platinum(II) complexes containing two or more different platinum(II) units connected by covalent bonds, Pt–Pt interactions can occur both within and between molecules. On account of the molecular structure of cyclometalated platinum(II) complexes, and whether intramolecular or intermolecular Pt–Pt interactions take place, this review roughly categorizes them into three types (Fig. 6). In the first type of molecules (**Pt82–Pt86**), we focus on structures with rigid connecting units between metal centers, which prevent intramolecular Pt–Pt interactions.[32,84–87] For example, in 2008, Che *et al.* reported an AIE polynuclear cyclometalated

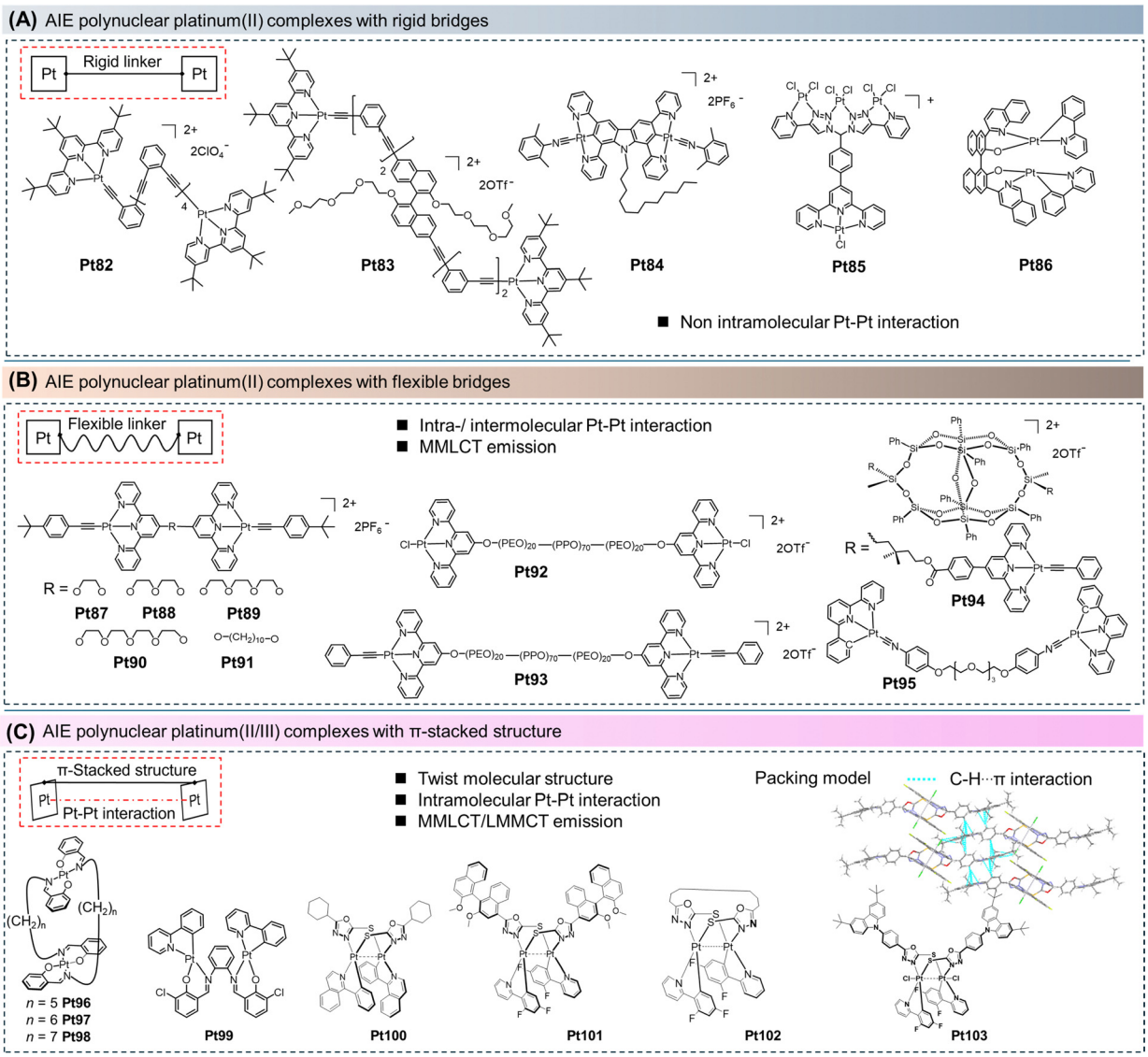

Fig. 6 (A) AIE polynuclear platinum(II) complexes with rigid bridges. (B) AIE polynuclear platinum(II) complexes with flexible bridges. (C) Molecular structures, single crystal structures, stacking modes of AIE platinum(II/III) complexes with π-stacked structures.

platinum(II) complex (**Pt82**, Fig. 6A) based on bridging ligands of *ortho*-phenylethynyl with a partially folded molecular conformation.[84] **Pt82** displayed an evident AIE phenomenon in an acetonitrile/H_2O system. The emission intensity increased and the emission wavelength red-shifted from 567 nm to 670 nm when the water content exceeded 40%. The single-crystal structure, dynamic light scattering, and transmission electron microscopy collectively revealed that **Pt82** aggregated into nanoparticles in the acetonitrile/H_2O mixture, with the *ortho*-phenylethynyl bridging ligand undergoing hydrophobic folding.

In the second type of molecules, our attention is paid to structures with flexible connecting units between metal centers, allowing for the possibility of intramolecular Pt–Pt interactions (**Pt87**–**Pt95**).[23,88–90] These complexes may exhibit dual emission features from mononuclear and binuclear excited states, impacted by a range of environmental factors such as temperature, polarity, and charged particles. For instance, Yam *et al.* reported a series of binuclear alkyne-bridged platinum(II) terpyridine complexes (**Pt87**–**Pt91**, Fig. 6B) in 2006, where two platinum(II) units were connected by a flexible bridge.[88] This work studied the intramolecular aggregation properties in solution. **Pt87** and **Pt88** with shorter connecting chains did not undergo self-aggregation or aggregation at room temperature. Conversely, **Pt89**–**Pt91** with longer flexible bridges could readily self-aggregate and aggregate in solution, and **Pt90** and **Pt91** were more prone to aggregation than the shorter chain **Pt89**. Thus, at room temperature, the solution of **Pt89**–**Pt91** was primarily intramolecularly aggregated, while dissociation occurred upon heating the sample. This study also demonstrated that Pt–Pt and π–π interactions could be regulated by temperature. In 2011, the group further replaced the central

flexible bridge with a triblock copolymer unit and synthesized AIE-active binuclear platinum(II) complexes (**Pt92** and **Pt93**, Fig. 6B) based on the terpyridine ligand.[23] They aggregated through Pt–Pt and/or π–π interactions at elevated temperatures. Transmission electron microscopy and dynamic light scattering studies revealed that above the critical micelle temperature, the presence of the block copolymer induced the formation of spherical micelles, leading to the observation of the AIE phenomenon.

In the third type of molecule, the entire molecule adopts a rigid π-stacking structure through bridging ligands and cyclometalated ligands. This π-stacking conformation is favorable for ground-state and/or excited-state interactions between the metal and/or its aromatic ligands (**Pt96–Pt103**).[22,37,91,92] For example, in 2011, Naota *et al.* reported a series of ''sandwich-type'' binuclear platinum(II) complexes (**Pt96–Pt98**, Fig. 6C) based on Schiff base ligands.[22] This work demonstrated the gelation of cyclohexane solutions with **Pt96–Pt98** induced by ultrasound, enabling precise control over phosphorescence emission. The specific process and mechanism will be explained in the following sections. In 2019, Xiang *et al.* reported a novel π-stacking AIE-active binuclear platinum(II) complex (**Pt99**), which revealed an apparent AIE effect in a mixed solvent of THF/H_2O.[91] Due to the hindered intramolecular rotation of the bridging Schiff base ligands, the π-stacking **Pt99** displayed strong intramolecular Pt–Pt interactions (3.37 Å) and powerful intermolecular interactions, such as C–H···π, C–H···O, and C–H···Cl interactions, resulting in a high solid-state PLQY of 35% (room temperature). Through the utilization of a nonchiral ligand, specifically 1,3,4-oxadiazole-2-thiol, to bridge two planar cyclometalated platinum(II) complexes, an enantiomeric pair of racemic *R*/*S* planar chiral binuclear platinum(II) complexes (referred to as **Pt100**) was successfully synthesized. Additionally, by using chiral (*R*)-/(*S*)-binaphthyl-derived ligands, enantiomerically pure *R, R, R*, or *S*, *S*, *S* complex (**Pt101**) could be prepared with 99% enantiomeric selectivity without the need for chiral HPLC separation. For **Pt100**, and **Pt101**, the cyclohexane or naphthyl groups on the peripheral bridging ligands can act as molecular rotors, allowing the molecules to dissipate energy through nonradiative pathways.[37] Thus, polynuclear platinum(II) complexes can be constructed in various ways and exhibit photoelectric properties that are different from those of mononuclear platinum(II) complexes. They have great application prospects in the field of NIR OLEDs and multi-stimulus response. However, how to further efficiently fabricate polynuclear platinum(II) complexes or polynuclear multi-metal complexes with high yield will be the focus of future research.

2.6.2 Polynuclear platinum(III) small molecules. Cyclometalated platinum(III) complexes are commonly used in catalytic reactions, yet, there have been few reports on their luminescent properties so far. Typically, binuclear platinum(III) complexes exhibit short-lived lowest triplet states, resulting in very weak or no phosphorescence. Additionally, platinum(III) complexes with low luminescence efficiency primarily undergo metal-centered transitions as the lowest electronic excited state. Interestingly, binuclear platinum(III) complexes with a d^7–d^7 electron configuration and an octahedral coordination structure possess several attractive features. For example, in 2020, Zhu *et al.* first reported an AIE binuclear platinum(III) complex (**Pt103**) with donor–acceptor-type bridging auxiliary ligands.[19] They proposed and validated the phosphorescence mechanism of these binuclear platinum(III) complexes, breaking the traditional non-luminescent behavior of platinum(III) complexes and achieving room-temperature multiple phosphorescence of platinum(III) complexes (Fig. 6C). According to the single-crystal structure, first, the corresponding spatial structures facilitate a reduction in intermolecular interactions (such as π–π stacking), thereby weakening the ACQ effect. Additionally, there were numerous weak intermolecular interactions, such as C–H···π and hydrogen bonding, which effectively inhibited nonradiative transitions, imparting AIE properties to the complex in the aggregate state.

3. Mechanisms

3.1 Restriction of intramolecular motion

As is well known, RIM is the main mechanism behind the AIE properties.[2,3,5] Like AIE fluorescent molecules, AIE cyclometalated platinum complexes consist of luminescent molecules with rotatable moieties (rotors) that undergo low-frequency rotation or torsional motion in dilute solutions. These motion modes lead to the dissipation of energy from the excited state triplet excitons through nonradiative transitions.[6–8] In the aggregated state, molecular motion is restricted due to steric hindrance and weak intermolecular interactions, resulting in the manifestation of the AIE phenomenon (Fig. 7). For instance, In 2023, Zhang *et al.* reported a cyclometalated platinum(II) complex (**Pt12**, Fig. 7A) with a 5/6/6 ring system.[16] This molecule possesses a more flexible molecular structure compared to the 5/5/6 ring cyclometalated platinum(II) complexes. The six-membered ring can undergo up-and-down vibrations, resulting in weak luminescence in dilute DMSO solution (5×10^{-5} mol L^{-1}) with a PLQY of less than 1%. However, when a poor solvent like water is introduced into the system, the classic AIE phenomenon is observed. At a water content of 70%, the PLQY of the system reaches 73.2%. Once the system forms aggregates, numerous weak intermolecular interactions restrain molecular vibrations and rotations, effectively suppressing nonradiative decay and exhibiting the AIE phenomenon (Fig. 7A). For other cyclometalated platinum(II) complexes with two-ligand (**Pt22**, Fig. 7B)[17] and three-ligand molecular frameworks (**Pt104**, Fig. 7C),[18] it is crucial to inhibit intermolecular π–π stacking, which requires the introduction of bulky steric hindrance groups. Furthermore, the rational introduction of heteroatoms (such as O, S, F, Cl, and N) increases various weak intermolecular interactions, further suppressing nonradiative transitions and imparting AIE effects to the complexes.

In 2020, Zhu *et al.* synthesized a three-dimensional binuclear cyclometalated platinum(III) complex (**Pt103**, Fig. 7D) with

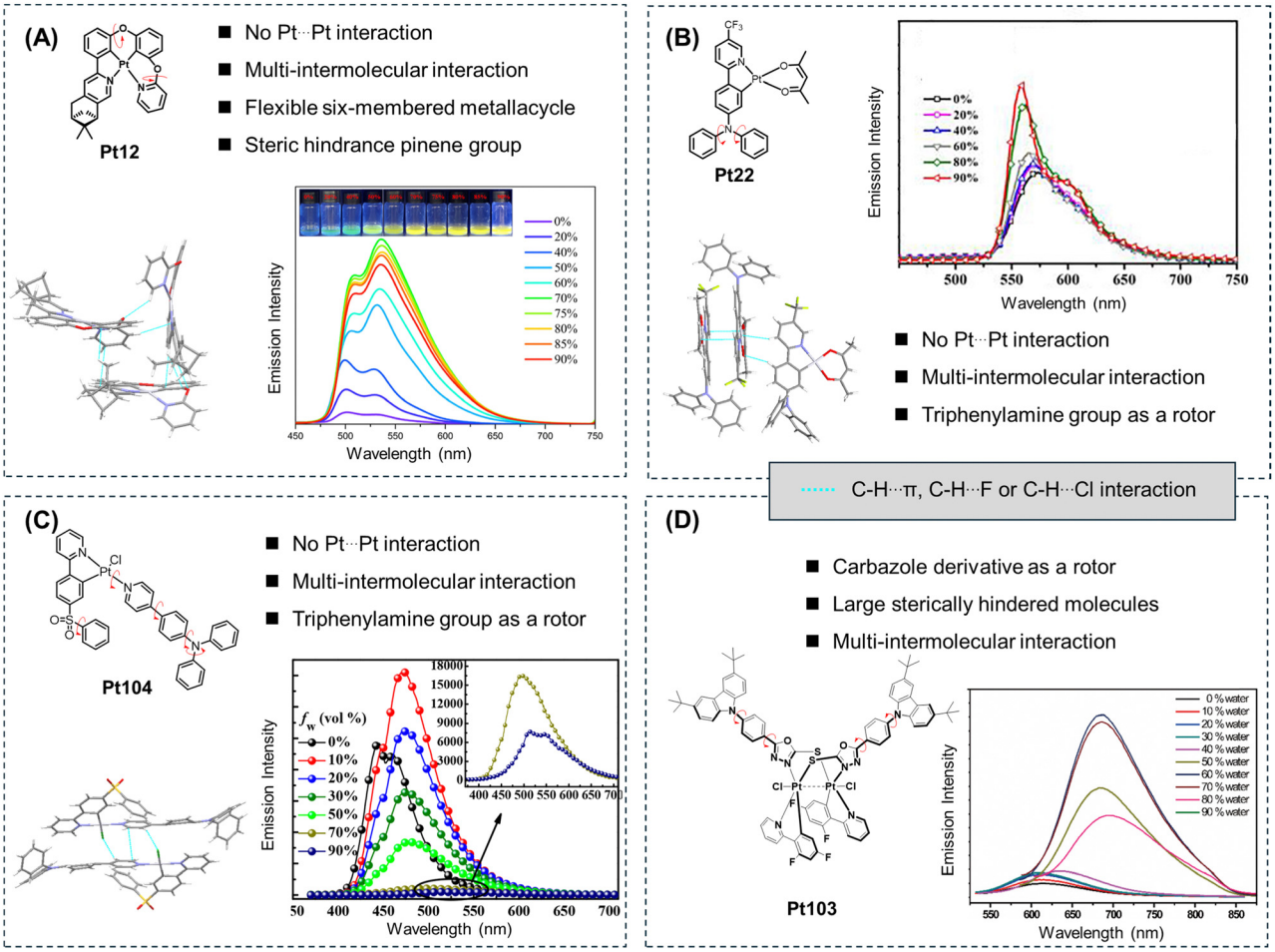

Fig. 7 Molecular structures, single crystal structures, stacking modes, and AIE curves of AIE cyclometalated platinum complexes with (A) one-ligand molecular frameworks, (B) two-ligand molecular frameworks, (C) three-ligand molecular frameworks, and (D) polynuclear platinum(III) with π-stacked structures. Reprinted with permission from (A) ref. 16, (B) ref. 17, (C) ref. 18 and (D) ref. 19. Copyright 2022 and 2021 Elsevier Ltd and 2018 and 2020 American Chemical Society, respectively.

AIE properties. **Pt103** possesses multiple molecular rotors, resulting in weak luminescence in dilute THF solution.[19] However, when a non-polar solvent like water is introduced into the system, the molecules undergo a certain degree of aggregation, producing enhanced emission and exhibiting a pronounced AIE phenomenon. The single-crystal structure of the molecule reveals that, due to steric hindrance effects, there is no π–π stacking between the molecules, thus effectively suppressing the ACQ phenomenon. Additionally, the various weak intermolecular interactions between the molecules reduce the nonradiative decay pathways in the aggregated state, resulting in the observed AIE phenomenon (Fig. 6C). Compared to other cyclometalated platinum complexes, the energy gap law and its impact on luminescence should be taken into consideration for polynuclear platinum complexes, especially in the NIR region.[33–35] So far, the RIM mechanism can explain the AIE phenomenon of most molecules. However, the RIM mechanism is more like the result of molecules producing the AIE phenomenon. Subsequently, we need to consider the specific reasons that cause RIM to further grasp the essence of the AIE properties. In future investigations of the AIE mechanism of cyclometalated platinum complexes, it is essential to delve deeper into these mechanisms and conduct more in-depth studies.[5]

3.2 Pt–Pt interactions

In cyclometalated platinum complexes, Pt–Pt interactions are a new class of intermolecular interactions that can effectively regulate the molecular self-assembly process and give rise to completely different photophysical properties in the aggregated state compared to the initial state.[20,21] The AIE phenomenon is one specific manifestation of the self-assembly process of these platinum complexes (Fig. 8). In 2002, Yam *et al.* first reported a cyclometalated platinum(II) complex (**Pt25**, Fig. 8A), which was modified with alkynyl groups to enhance the solubility of the molecule.[10] They investigated the self-assembly behavior of **Pt25** in diethyl ether/acetonitrile solution through Pt–Pt interactions. It revealed that upon the addition of a non-polar solvent diethyl ether to the acetonitrile solution of **Pt25**, the color changed from yellow to green and then to blue,

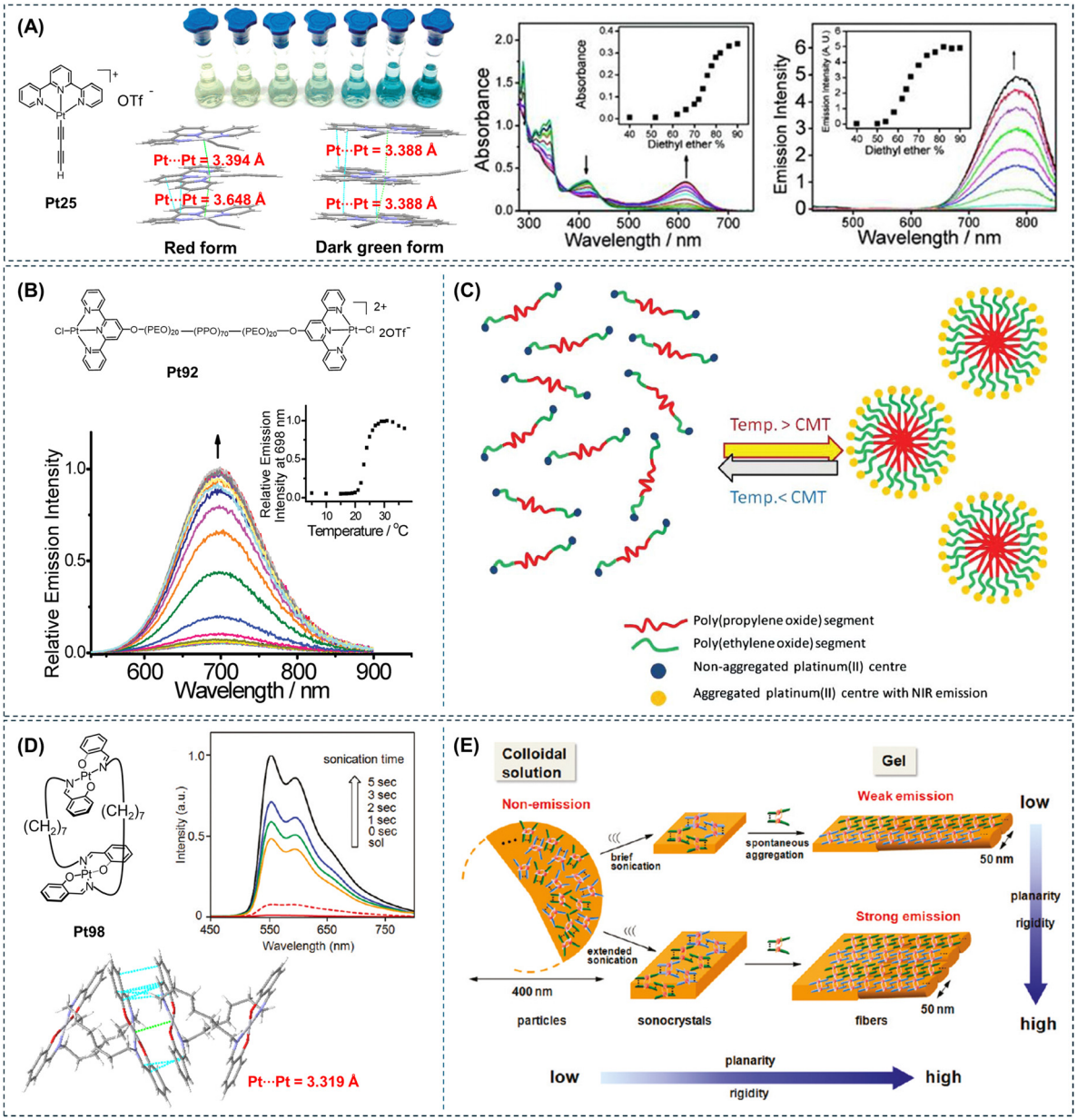

Fig. 8 (A) Molecular structure and single molecular stacking modes of **Pt25**, color change of **Pt25** in acetonitrile solution upon increasing the ether, UV-visible and emission spectral changes of **Pt25** in acetonitrile solution upon gradual addition of ether fraction. Reproduced with permission from ref. 10. Copyright 2002, American Chemical Society. (B) Molecular structure of **Pt92**, emission of **Pt92** at different temperatures. (C) Schematic diagram of the aggregation of platinum(II) complexes due to micellization at above the critical micelle temperature of the PEO–PPO–PEO block copolymer. Reproduced with permission from ref. 23. Copyright 2011, Royal Society of Chemistry. (D) Molecular structure and single molecular stacking modes of **Pt98**, emission changes of **Pt98** upon sonication, and (E) schematic diagram of the aggregate morphology and conformational changes of **Pt98** during the ultrasound-induced gelation process. Reproduced with permission from ref. 22. Copyright 2011, American Chemical Society.

accompanied by NIR emission (Fig. 8A). These intriguing photophysical properties were attributed to the directional Pt–Pt interactions formed during the self-assembly and aggregation process of the complex, eliciting enhanced MMLCT absorption and ^{3}MMLCT emission and inducing the classical AIE phenomenon. In cyclometalated platinum complexes, Pt–Pt interactions are a new class of intermolecular interactions that can effectively regulate the molecular self-assembly process and give rise to completely different photophysical properties in the aggregated state compared to the initial state.[20,21] The AIE phenomenon is one specific manifestation of the self-assembly process of these platinum complexes.

In 2011, Yam *et al.* further reported a binuclear platinum(II) complex (**Pt92**, Fig. 8B) based on a tridentate pyridine ligand.[23] The emission peak of **Pt92** in the water solution was located at 698 nm. The emission intensity exhibited limited sensitivity to variations in temperature below 21 °C. However, as the temperature surpassed 21 °C, a gradual increase in emission

intensity was observed, with the most notable enhancement occurring around 23 °C, corresponding to the lower critical solution temperature of the triblock copolymer in **Pt92**. The emission intensity saturated at around 31 °C, and further temperature increase led to a decrease in emission intensity (Fig. 8B). Within the temperature range of 15 to 31 °C, the temperature increase likely induced the formation of polymer micelles, which brought the platinum(II) tridentate pyridine groups into proximity through intramolecular or intermolecular Pt–Pt interactions, resulting in observed MMLCT transitions and emission arising from the aggregation (Fig. 8C).

In 2011, Naota *et al.* reported a clothespin-shaped binuclear platinum(II) complex (**Pt98**, Fig. 8D) based on Schiff base ligands.[22] **Pt98** emitted rapid and intense luminescence upon ultrasound-induced gelation in cyclohexane, demonstrating an ultrasound-induced emission phenomenon. The formed luminescent gel was stable at room temperature but easily reverted to the initial non-luminescent solution upon heating above the gelation temperature. The single-crystal structure of **Pt98** revealed that due to the overall clothespin-shaped structure of the molecule, the Schiff base portion of the complex adopted a planar quadrilateral structure. There was a π–π stacking arrangement between the molecules, with a Pt–Pt distance of 3.319 Å (Fig. 8D). Based on the experimental results, the mechanism of the ultrasound-induced gelation process was elucidated in Fig. 8E. Under non-ultrasound conditions, **Pt98** formed colloidal particles in solution through loose and non-penetrating intermolecular stacking. Imposing ultrasound energy to these particles induced the formation of microcrystals. Further ultrasound treatment disrupted the obtained ultrasound crystals and induced spontaneous anisotropic growth of flexible gel fibers. Under non-ultrasound conditions, the weak emission of colloidal particles was owing to the loose aggregation state of the molecules, allowing **Pt98** to undergo non-radiative transitions and dissipate energy. After ultrasound treatment, the loose stacking of **Pt98** units in the colloidal solution transformed into rigid, inward stacking in the gel fibers. This morphological change dramatically reduced the average mobility of each monomer unit, thereby suppressing energy loss in phosphorescence emission. In this work, the Pt–Pt interaction acts as an important driving force for the self-assembly and aggregation of planar platinum complexes. The AIE phenomenon of this type of molecule can also be termed as self-assembly-induced emission/enhancement. Utilizing the different excited states formed after molecular aggregation to emit light provides us with a new perspective to further study the luminescence behavior of aggregates.[21]

3.3 Restricted distortion of the excited-state structure

The principle of restricted molecular excited-state distortion was proposed by Huang *et al.* in 2012.[24] This mechanism applies to the AIE cyclometalated platinum(II) complex with phenyl-pyridine and Schiff base ligands, as illustrated in Fig. 9. The authors synthesized a series of molecules, taking **Pt17** and **Pt20** as examples. It was observed that both complexes did not emit light in the solution state but exhibited completely different phenomena in the crystalline state. **Pt17** emitted strong light in the crystal form, displaying an AIE effect, while **Pt20** remained non-emissive without AIE behavior (Fig. 9A). Since these two molecules have similar structures and both possess molecular rotors, the RIM mechanism may not be responsible for the AIE phenomenon observed in **Pt17**. So, the authors conducted theoretical calculations and found that in the excited states of both molecules in solution, the LUMO electron clouds were only distributed on the platinum ions and the Schiff base ligands, without distribution on the phenyl-pyridine moiety. This could be one of the reasons why these two molecules did not emit light in the solution state (Fig. 9B). Additionally, in the solution state, there was a significant deformation of the molecular configuration in the T_1 excited state of both molecules. The energy of the excited state was dissipated through molecular distortion *via* non-radiative transitions, leading to non-emission (Fig. 9B). In contrast, in the crystalline state, the LUMO electron cloud of **Pt17** in the excited state was distributed on both the phenyl-pyridine and Schiff base ligands, with the involvement of the phenyl-pyridine ligand in light emission (Fig. 9C). Meanwhile, the authors found that the deformation of the excited state in **Pt17** was restricted in the crystalline state, leading to strong emission. However, the phenyl-pyridine moiety in **Pt20** still did not participate in emission (Fig. 9D).[24,25]

3.4 Restriction of coordination skeletal deformation

In comparison to traditional platinum(II) complexes, cyclometalated platinum(II) complexes with a three-ligand framework allow easy rotation of two independent monodentate ligands. According to the RIM mechanism, the weak emission of these platinum(II) complexes in solution can be attributed to intramolecular bond rotation, promoting nonradiative decay and significantly reducing the PLQYs. On the other hand, the strong emission in the aggregated state results from the restriction of intramolecular bond rotation, leading to a significant reduction in nonradiative decay. However, recent studies have shown that the molecular structure in the excited state is crucial for understanding the fundamental working mechanism of AIE-active emitters.[26–28]

In 2020, Wong *et al.* developed a platinum(II) complex (**Pt105**, Fig. 10) with a three-ligand framework.[77] **Pt105** displayed minimal emission in dichloromethane solution ($\approx 2 \times 10^{-5}$ mol L^{-1}) with a PLQY of only 0.8%. However, it emitted bright blue-green light in doped films (PMMA film doped with ≈1.0 wt% platinum complex at room temperature, PLQY = 29%) or the crystalline state, proving an evident AIE effect. The authors also explored the luminescence of **Pt105** under different THF/H_2O volume ratios, further confirming its AIE properties (Fig. 10E). After that, the authors first obtained the optimized molecular configurations of the ground state (S_0), singlet state (S_1), and triplet state (T_1) of **Pt105** through theoretical calculations. The ground state configuration of **Pt105** exhibited an overall planar structure, as shown in Fig. 10A, with a dihedral angle of only 2.7° between the yellow plane P1 (containing Pt ions, C2, and N2) and the blue plane P2

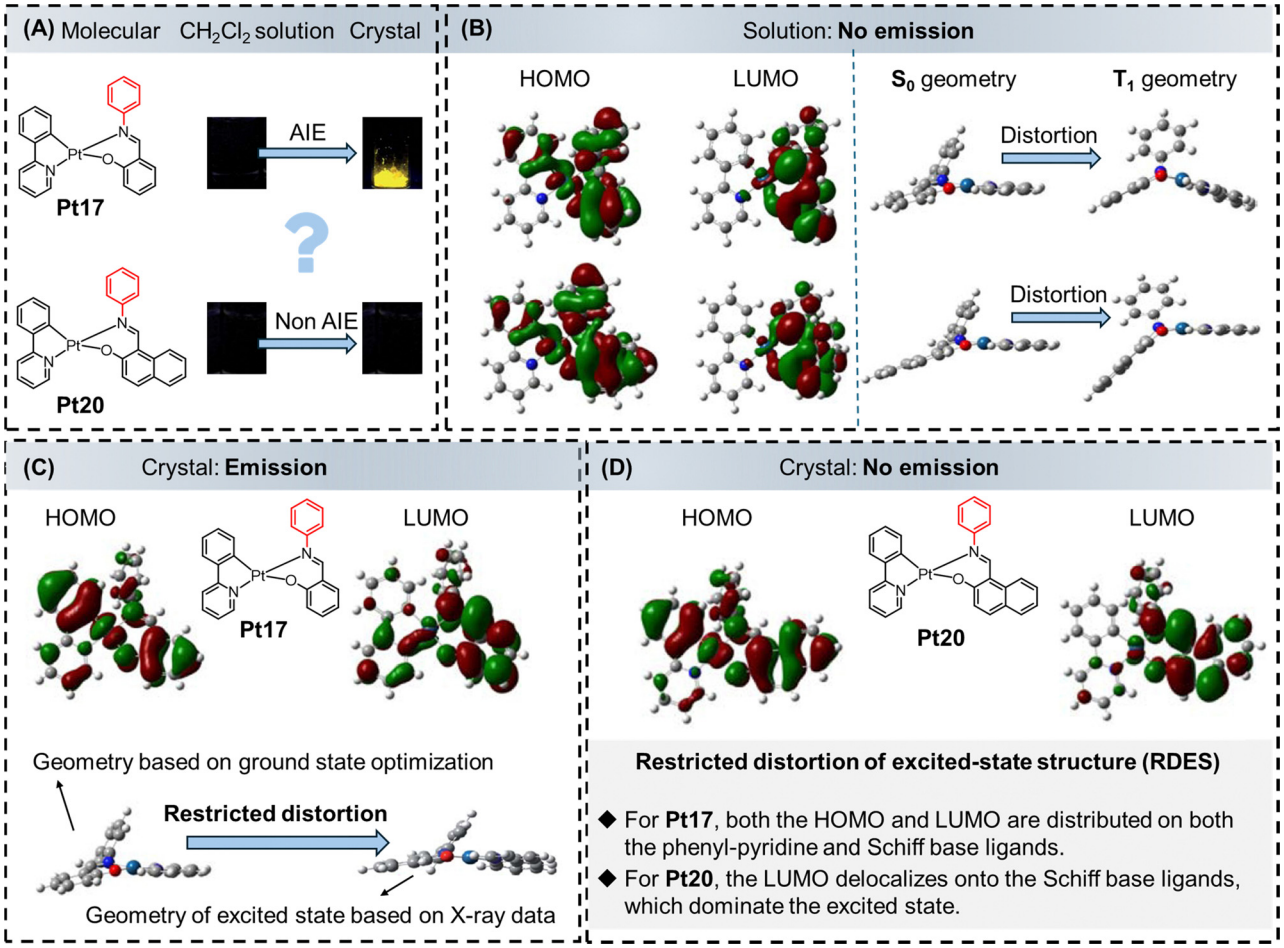

Fig. 9 AIE mechanism based on the restricted distortion of the excited-state structure. (A) Molecular structures of **Pt17** and **Pt20**, luminescence photographs of **Pt17** and **Pt20** in CH_2Cl_2 solution and crystal state. (B, left) HOMO and LUMO distributions of **Pt17** and **Pt20** (gas state) at the excited state. (B, right) The optimized ground-state and triplet-state geometries of **Pt17** and **Pt20**. (C) Calculated geometries and molecular orbitals of **Pt17** in different states (based on the corresponding crystal structures). (D) The calculated HOMOs and LUMOs of **Pt20** at the triplet state (based on the corresponding crystal structures). Reprinted with permission from ref. 24. Copyright 2012 Royal Society of Chemistry.

(containing Pt ions, C1, and N1). In the S_1 state, the molecular structure underwent a significant change, transitioning into a tetrahedral configuration, with a dihedral angle of 43.2° between P1 and P2 (Fig. 10B). For the T_1 state, it reverted to a planar structure, with a dihedral angle of 3.3° between P1 and P2 (Fig. 10C). Furthermore, Fig. 10D represents the linear interpolated internal coordinate (LIIC) pathway of **Pt105**. In the solution state, the molecule can easily reach the minimal energy conical intersection (MECI) between S_0 and S_1 when excited by light. At the same time, the intersystem crossing (ISC) efficiency from S_1 to T_1 is low in solution, and the molecule undergoes a process of coordination framework deformation, achieving the S_1 to S_0 transition through ultrafast internal conversion (IC) *via* non-radiative transitions, resulting in the non-emissive behavior of **Pt105** in solution. In the aggregate state, the restriction of coordination skeletal deformation would significantly enhance the energy gap between S_1 and S_0 at the MECI and reduce the rate of the IC process. Moreover, the T_1 state exhibited a planar geometry similar to the S_0 state at the Frank-Condon point, facilitating efficient ISC from S_1 to T_1 and promoting emission from the T_1 state.[77] In 2021, Zhou *et al.* further reported a model molecule (**Pt106**, Fig. 10F) with AIE properties in THF/H_2O solution and proposed a new mechanism of AIE, named restrained D_{2d} deformation of the coordinating skeleton.[29] As shown in Fig. 10G, similar to the RCSD mechanism, in the solution state, molecules dissipate energy through non-radiative transitions by undergoing structural deformations, resulting in non-emission. In the aggregated state, the deformation of the square planar (D_{4h}) coordinating skeleton to tetrahedron (T_d) is restricted, promoting the radiative transition of excitons and thus exhibiting AIE characteristics.[29]

3.5 Restriction of molecular configuration transformation

Choosing an appropriate molecular model is crucial to study the AIE mechanism of platinum complexes. In 2023, Zhao *et al.* reported the simplest *cis*-bis(2-phenylpyridine) platinum(II) complex (**Pt107**, Fig. 11).[30] **Pt107** was non emissive in dilute DMSO solutions. However, they produced intense red and deep-red phosphorescence in the film states (doping

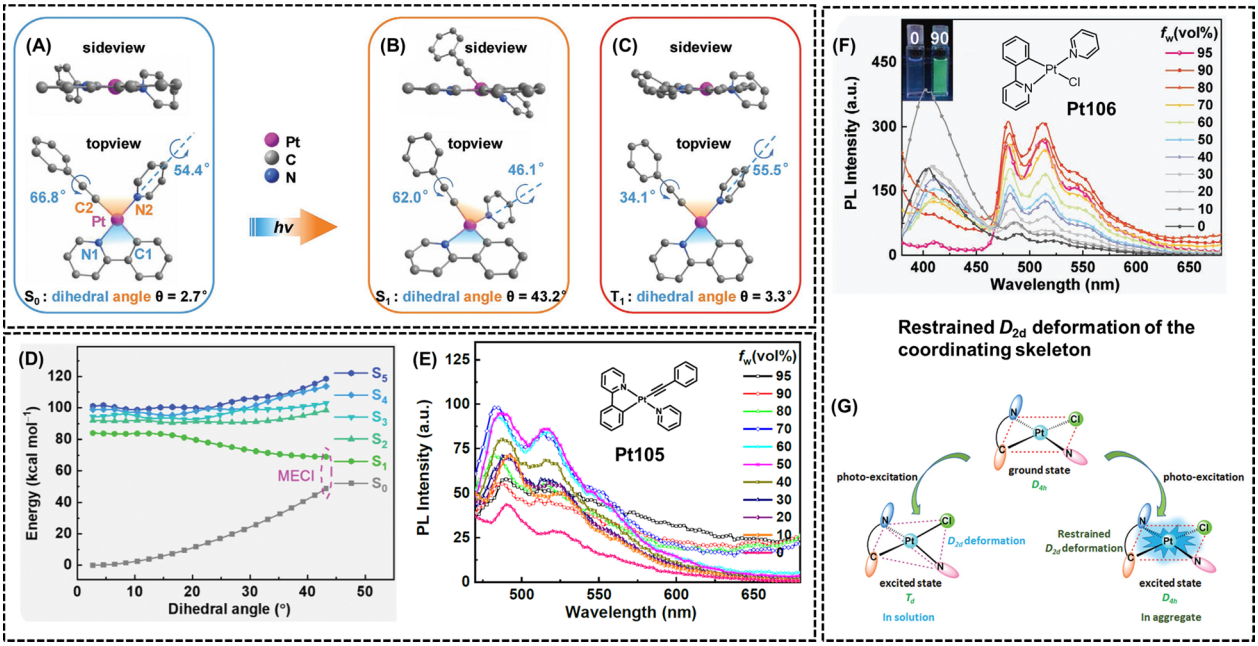

Fig. 10 AIE mechanisms based on the restriction of coordination skeletal deformation and restrained D_{2d} deformation of the coordinating skeleton. Optimized structures of **Pt105** at (A) S_0 minimum, (B) S_1 minimum, and (C) T_1 minimum (hydrogen atoms are omitted for clarity). (D) The calculated LIIC pathway from the Frank–Condon point to the MECI of **Pt105**. Molecular structures and AIE curves of (E) **Pt105** and (F) **Pt106**. (G) Proposed AIE mechanism of the restrained D_{2d} deformation in **Pt106**. Reprinted with permission from (A)–(E) ref. 77, and (F) and (G) ref. 29. Copyright 2020 Wiley-VCH, and 2021 Royal Society of Chemistry, respectively.

concentration of 5 wt% in PMMA), with PLQY up to 69.4%, exhibiting unique AIE characteristics. Then, the authors also obtained the optimized molecular configurations of S_0, S_1, and T_1 of **Pt107** through theoretical calculations (Fig. 11A). In the S_0 state, the molecule adopts a quasi-planar configuration, with a dihedral angle of 21.82° between the yellow plane and the blue plane (Fig. 11A). However, in the excited states (S_1 and T_1), the molecular configuration undergoes significant changes, with dihedral angles of 99.10° and 85.36°, respectively (Fig. 11A). Additionally, the platinum ion contributes more than 66% and 51% to the hole and particle orbitals, respectively (Fig. 11B). Therefore, in the excited states, d–d transitions in the metal center may lead to substantial molecular deformations. Fig. 11C illustrates the LIIC pathway of **Pt107**. So, it can be observed that in the solution state, the molecule can easily reach the MECI between S_0 and S_1 upon excitation, resulting in non-emission. In the aggregated state, various interactions between molecules, such as C–H···π and Pt–Pt interactions (Fig. 11D), limit the deformation of the excited state, suppressing non-radiative transitions and ultimately exhibiting the phenomenon of AIE.[30]

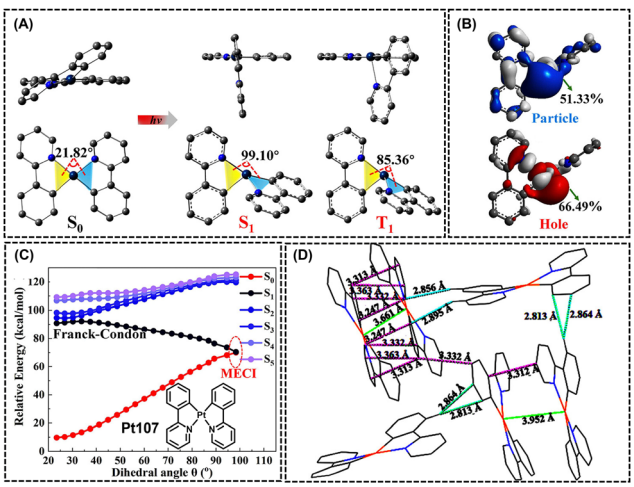

Fig. 11 AIE mechanism based on restriction of molecular configuration transformation. (A) Geometries for the S_0 and S_1 and T_1 states, obtained from the single-crystal structure and theoretical optimization, respectively. (B) Natural transition orbitals based on the optimized T_1 structure. (C) Molecular structure of **Pt107** and the relationships between the dihedral angles and the relative energies based on the LIIC pathway calculations. (D) Crystal packings and the intermolecular interactions of **Pt107**. Reprinted with permission from ref. 30. Copyright 2023 American Chemical Society.

By summarizing the AIE mechanisms, current research on the AIE mechanism of platinum complexes has gradually shifted towards the deactivation processes of the excited states. Table S2 (ESI†) provides a summary of the similarities and differences between mechanisms RCSD, restrained D_{2d} deformation of the coordinating skeleton, and RMCT. The non-emissive behavior of platinum complexes in the solution state can be attributed to the deactivation of the excited states through molecular deformations leading to non-radiative transitions. On the other hand, in the aggregated state, the restricted deformation of the excited-state molecular structure activates the radiative transition process, thereby exhibiting the phenomenon of AIE.

In addition to the AIE mechanisms, there are several other mechanisms as well. For example, in 2021, Zhong *et al.* synthesized and characterized a dimeric platinum(II) complex (**Pt84**, Fig. 6A) with a rigid planar carbazole bridge. The design of **Pt84** aimed to incorporate multiple non-covalent interaction sites to regulate the aggregation behavior of the molecule, including Pt–Pt interactions (Pt–Pt distance of only 3.408 Å), π–π interactions from the carbazole bridge and terminal aromatic groups, as well as hydrophobic/hydrophobic interactions from alkyl substituents on the carbazole nitrogen atoms. Based on the analysis of the single crystal structure, as well as phosphorescence lifetime testing and PLQY testing in a nitrogen or air atmosphere, the AIE phenomenon is considered being caused by the oxygen-shielding effect and the molecular rigidification-induced decrease of nonradiative decays in the aggregate state.[32]

4. Applications

4.1 Biological imaging and therapy

Compared to traditional ACQ molecules, AIE molecules have been designed with high PLQY, excellent photostability, and outstanding biocompatibility. AIE molecules have been successfully employed in cellular imaging and *in vivo* diagnostics.[2–4,93] Some AIE molecules possess remarkable ROS generation capability or efficient photothermal conversion efficiency, enabling fluorescence imaging-guided photodynamic therapy (PDT) or photothermal therapy (PTT) for cancer treatment.[94] Furthermore, by incorporating other anticancer drugs into therapeutic AIE molecular systems, image-guided combination therapy can be achieved to improve their therapeutic efficacy. Typically, transition metal complexes with cytotoxicity are used as therapeutic agents but lack diagnostic functionalities.[82] It is challenging to timely and on-site track the drugs without additional diagnostic agents. Therefore, combining transition metal complexes with AIE molecules is a promising strategy for constructing theranostic agents. Moreover, the introduction of transition metal atoms into AIE molecular systems, facilitated by the heavy atom effect, can promote the ISC process, stabilize the triplet excitons, and potentially enhance ROS generation.[38–40,83] For AIE platinum complexes, the performance of fluorescence imaging can be significantly improved by designing ligand structures and introducing platinum ions. This includes enhancing PLQY, red-shifting absorption, and emission wavelengths, prolonging luminescence lifetimes, and increasing Stokes shifts. Therefore, constructing AIE platinum complexes enables imaging of specific cells, responsive imaging of cellular/tumor microenvironments, activatable imaging of biological processes, and localized imaging of cells/tumor tissues. These applications provide new means for early detection and quantitative analysis of tumors (Fig. 12).[38–40,67,83]

As shown in Fig. 12A (left), in a study conducted in 2021, Yam *et al.* discovered that the incorporation of a guanidinium group into the platinum(II) complex (**Pt45**) facilitated noncovalent interactions between the complex and RNA, resulting in a notable increase in RNA affinity.[67] Remarkably, the aggregation affinities inherent in platinum(II) complexes allow for the manifestation of striking luminescence turn-on (MMLCT) upon RNA binding, stemming from the enhanced noncovalent interactions of Pt–Pt and π–π stacking. The complexes not only demonstrate captivating spectroscopic alterations and luminescence enhancement following RNA binding but also enable targeted nucleolus imaging within cellular environments. In comparison to fluorescent dyes, the low-energy red luminescence and significant Stokes shifts exhibited by platinum(II) complexes contribute to a heightened signal-to-background autofluorescence ratio, particularly advantageous for nucleolus imaging. The utilization of **Pt45** has been employed to track the dynamics of the nucleolus in response to the introduction of RNA synthesis inhibitors. This capability facilitates inhibitor screening and holds potential advantages in the development of anti-tumor drugs.

In 2022, Yam *et al.* further developed a tridentate cyclometalated platinum(II) complex (**Pt108**), which revealed significant concentration-dependent luminescence due to intermolecular Pt–Pt interactions and π–π stacking interactions.[95] As shown in Fig. 12A (right), as the solution concentration increases, the emission wavelength of the system can shift from green to red light. To delve deeper into the impact of complex concentration on the emission and localization of **Pt108** in live cells, co-localization experiments were conducted following the incubation of live HeLa cells with either 10 μM or 50 μM **Pt108**. When the incubation concentration was further increased to 50 μM, the co-localization of **Pt108** with lysosomes gradually disappeared. In contrast, targeting the cell nucleus occurred accompanied by the red emission signal within live HeLa cells, which further implies the concentration-dependent subcellular distribution behavior of **Pt108**. Moreover, the shorter incubation time (0.5 h) suggested that the monomeric state of **Pt108** can easily pass through the cell membrane and diffuse and accumulate inside the cells through passive diffusion. The accumulation of red emission in the cell nucleus was achieved by electrostatic interactions driven by the nuclear negative charge, and this accumulation further promoted the self-assembly of monomers. Therefore, **Pt108** exhibited unique subcellular redistribution and imaging capabilities from lysosomes to the cell nucleus in both live and dead cells (Fig. 12A).

Since cisplatin is approved for clinical treatment of solid tumors, numerous cisplatin analogs have been synthesized. Some cisplatin analogs have obtained clinical approval, such as lobaplatin, nedaplatin, carboplatin, oxaliplatin, and picoplatin. However, in practice, cisplatin and its analogs can cause adverse reactions such as nephrotoxicity and neurotoxicity. Their resistance may reduce the effectiveness of treatment, making them unsuitable for clinical use.[41,82,83] The four-ligand molecular framework of platinum(II) complexes has similar molecular structures to commercially available chemotherapeutic drugs such as cisplatin derivatives, making them suitable for tumor diagnosis and treatment.[41,83] As shown in Fig. 12B (left), in 2020, Liu *et al.* ingeniously integrated an

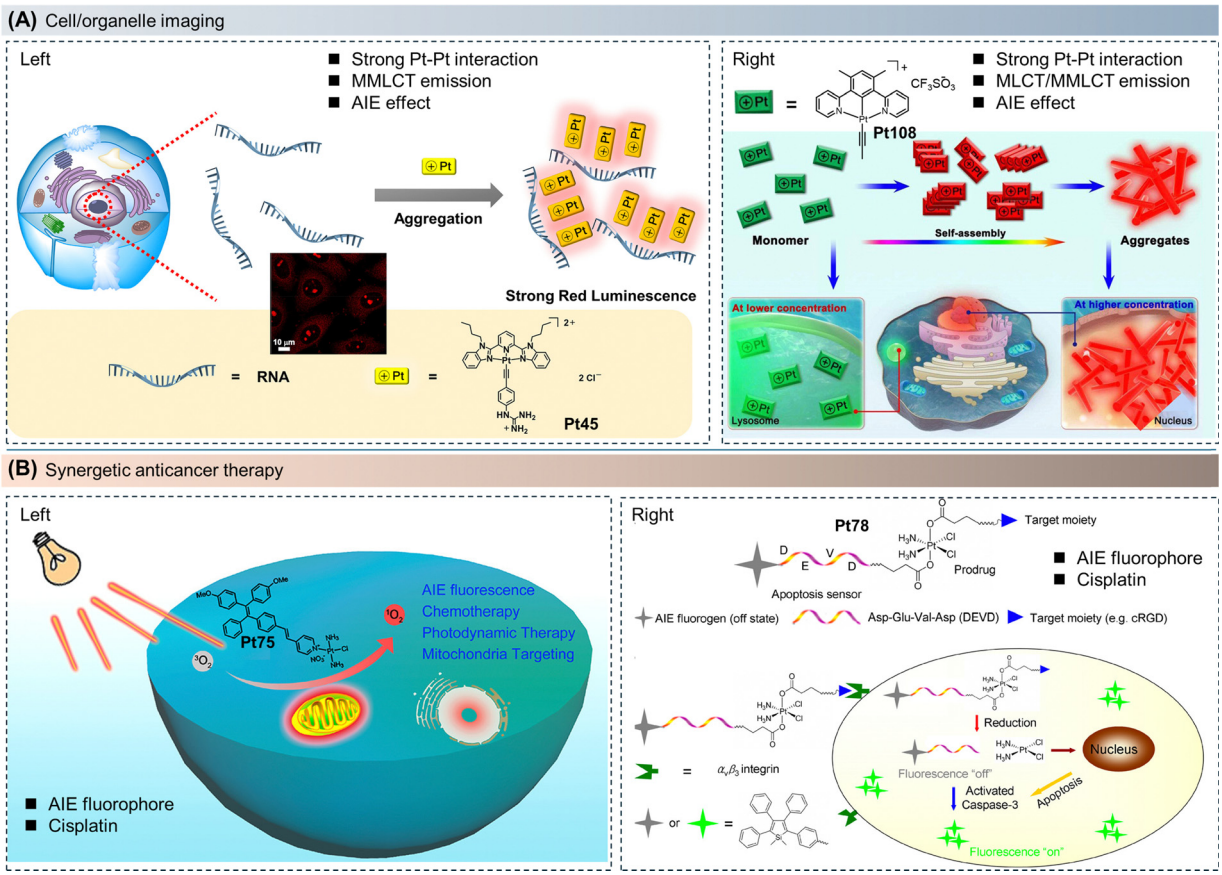

Fig. 12 Molecular structures and the schematic diagram of the mechanism of imaging and therapy. The applications of AIE platinum complexes in (A) cell/organelle imaging, and (B) synergetic anticancer therapy. Reprinted with permission from (A, left) ref. 67, (A, right) ref. 95, (B, left) ref. 41, and (B, right) ref. 38. Copyright 2021 American Chemical Society, 2022 Wiley-VCH, 2020 American Chemical Society, and 2014 American Chemical Society, respectively.

AIE fluorophore with cisplatin, synthesizing an AIE platinum(II) complex (**Pt75**) for synergistic anticancer therapy. By adjusting the donor structure coordinating with the cisplatin moiety, balancing hydrophobicity–hydrophilicity, donor–acceptor strength, and intramolecular charge transfer effects, the newly designed AIE photosensitizer, **Pt75**, can be effectively taken up by cells, exhibiting chemotherapy effects similar to cisplatin and superior ROS generation ability compared to 5,10,15,20-tetrakis(2-hydroxyphenyl)porphyrin (Ce6). Importantly, **Pt75** manifested synergistic photodynamic and chemotherapy effects on C6 glioma cells, showing 2.4-fold higher efficacy than cisplatin under white light irradiation (15 J cm^{-2}). The authors further conducted cell cycle analysis and apoptosis assays, which revealed that **Pt75** could synergistically inhibit DNA replication and induce cell apoptosis through its photodynamic and chemotherapy functions.[41]

Typically, platinum(IV) drugs are considered prodrugs of platinum(II) drugs. Compared to divalent cisplatin analogs, platinum(IV) drugs can reduce drug resistance in tumor cells and minimize toxicity to normal cells. To activate the anticancer ability of platinum(IV) complexes, various reductants such as metallothioneins, glutathione (GSH), ascorbic acid, and cysteine are required to reduce platinum(IV) to platinum(II).[38–40] To minimize the adverse reactions of platinum(II) drugs and enhance their anticancer activity, combining platinum(IV) complexes with photosensitive nanoparticles is an available method, which can significantly improve the bioavailability of platinum drugs, reduce adverse reactions, and overcome current resistance. In addition, by incorporating platinum(IV) complexes into the AIE molecular system, image-guided combination therapy can be achieved, enhancing both therapeutic and diagnostic capabilities while enabling timely and *in situ* tracking of the drug.[38–40]

Tumor-targeted drug delivery is an effective method for minimizing side effects, as cancer cells often overexpress certain membrane receptors, including integrin αvβ3, folate receptors, and glucose receptors. This provides a practical strategy for designing cancer-selective drugs. Platinum-based anticancer drugs typically induce apoptosis in cancer cells. To achieve real-time and non-invasive evaluation of the therapeutic outcomes of platinum(IV) prodrugs, as shown in Fig. 12B (right), Tang *et al.* developed **Pt78**. The AIE-active TPS is coordinated to the platinum(IV) center through a caspase-3 enzyme-specific peptide, DEVD (Asp–Glu–Val–Asp). With the presence of the cRGD peptide in the molecule, this platinum(IV) prodrug can be selectively taken up by U87-MG cancer cells

overexpressing αvβ3. Upon internalization into the cells, the active platinum(II) unit is released to trigger apoptosis and activate caspase-3. Subsequently, the activated caspase-3 cleaves TPS-DEVD, enhancing the AIE fluorescence of 1,1-dimethyl-2,3,4,5-tetraphenyl-1*H*-silole derivatives (TPS). Furthermore, in U87-MG cells, the fluorescence intensity induced by apoptosis is closely correlated with the prodrug concentration and cell viability. This built-in cellular apoptosis sensor enables cancer-targeted drug delivery and synchronous therapeutic feedback at the single-molecule level.[38]

In the field of biological applications, one aspect involves utilizing the red or NIR emission of platinum complexes in the aggregated state to achieve high-resolution imaging. The AIE properties of the molecules play a crucial role in overcoming the ACQ effect, thereby enhancing the luminescence efficiency. On the other hand, by constructing cisplatin-like drugs and utilizing their therapeutic effect on tumors, the AIE properties of the platinum complexes can enable real-time monitoring of the drugs and treatment efficacy, thereby achieving integrated diagnosis and therapy.

4.2 Optoelectronics

Organic light-emitting diodes, abbreviated as OLEDs, are considered the next generation of display and lighting technology due to their lightweight, flexibility, high efficiency, and wide viewing angles. Cyclometalated platinum complexes, as classical phosphorescent materials, have a 100% utilization efficiency of excitons, making them widely used in constructing efficient OLEDs.[96] It is worth noting that the fabrication of optoelectronic devices usually involves techniques such as vapor deposition or spin-coating. Therefore, the thermal stability of the emitters must meet the device preparation requirements. Similar to common ACQ fluorophores, cyclometalated platinum complexes may also exhibit ACQ phenomena, which greatly hinder their application in OLEDs. Therefore, the development of cyclometalated platinum complexes with AIE properties is of great importance and has witnessed rapid progress in recent years.[2,6–8]

As mentioned earlier, homoleptic bidentate ligand platinum(II) complexes possess excellent molecular rigidity, high PLQY, and self-assembly properties, which are suitable for constructing efficient OLEDs.[33–36] Chi *et al.* designed a series of square planar platinum(II) complexes, including **Pt13**, **Pt14**, **Pt109**, and **Pt110**, to reduce the nonradiative transitions of the molecules through exciton delocalization and molecular deuteration, leading to a range of efficient near-infrared cyclometalated platinum(II) complexes (Fig. 13A).[33–36] These complexes formed crystalline aggregates in thin films deposited by vapor deposition. Grazing-incidence X-ray diffraction effectively characterized the stacking geometry, revealing a domino-like packing arrangement with intermolecular π–π distances of 3.4–3.7 Å. To confirm the presence of exciton delocalization, the authors employed time-resolved step-scan Fourier-transform ultraviolet-visible spectroscopy to probe the exciton delocalization length of the platinum(II) aggregates, which ranged from 5 to 9 molecules (2.1–4.5 nm) predominantly along the π–π stacking direction (Fig. 13A).[34]

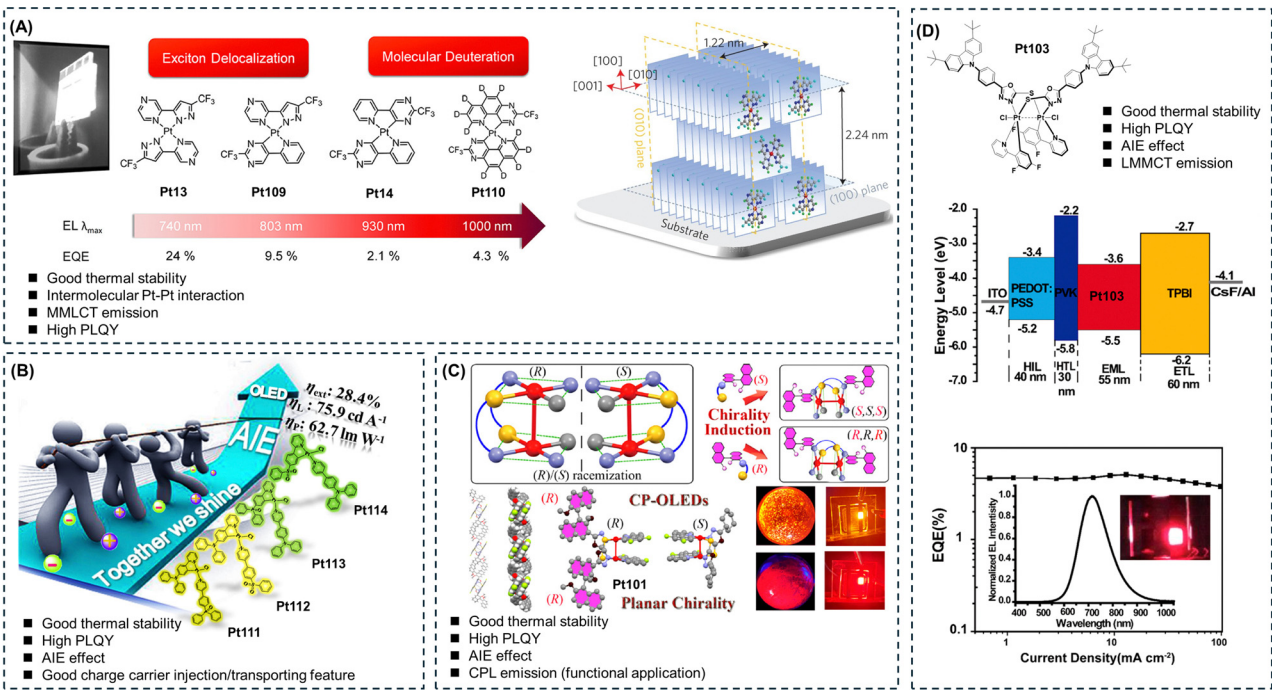

Fig. 13 Molecular structures, device structures, and performances in optoelectronics applications. The applications of AIE cyclometalated platinum complexes with (A) two-ligand frameworks, (B) three-ligand frameworks, (C) polynuclear platinum(II) with π-stacked structures, and (D) polynuclear platinum(III) with a π-stacked structure in optoelectronics. Reprinted with permission from (A) ref. 33, (B) ref. 18, (C) ref. 37, and (D) ref. 19. Copyright 2023, 2018, 2022, and 2020 American Chemical Society, respectively.

To investigate the isotope effect, fully deuterated platinum(II) complex **Pt110** was synthesized.[36] It was found that the vapor-deposited films of fully deuterated platinum(II) complex exhibited the same emission peaks as the non-deuterated platinum(II) complex but with an approximately 50% increase in PLQY. To translate the fundamental research into practical applications, the authors incorporated these NIR platinum(II) complexes into OLEDs as emitting layers, achieving external quantum efficiencies (EQE) as high as 2–25%. Although the mentioned work did not explicitly address the AIE properties of the complexes and did not employ the traditional solvent-induced method to study the molecular AIE performance, it provided an approach for further investigating the aggregation behavior of molecules in the solid state, particularly in thin film states.[33–36]

The platinum(II) complexes with a three-ligand molecular framework effectively suppress the π–π interactions observed in traditional cyclometalated platinum(II) complexes, thereby improving the balance of electron and hole injection/transport behaviors.[18,26,28,29] Consequently, they have been broadly utilized in OLEDs in recent years. In 2018, Zhou *et al.* fabricated a class of highly efficient cyclometalated platinum(II) complexes (**Pt111**–**Pt114**, Fig. 13B), as emitters in solution-processed phosphorescent OLEDs.[18] Among them, the device based on **Pt114** as the emitter attained an EQE as high as 28.4%. The results realized by these complexes should provide valuable clues for exploring AIE-active phosphorescent platinum(II) complexes with high EL performance.

In addition to AIE mononuclear platinum(II) complexes, π-stacked polynuclear AIE cyclometalated platinum(II) complexes have been widely employed in exploiting near-infrared OLEDs due to their rigid three-dimensional stereochemistry and strong ^{3}MMLCT effect.[37,92] In 2022, Xiang *et al.* synthesized and characterized a soft-bridged dinuclear platinum(II) complex, **Pt101**, with metal-induced planar chirality (Fig. 13C).[37] **Pt101** displays strong red circularly polarized phosphorescence with PLQY of up to 80.3% (doping concentration of 10 wt% in *m*CP) and can be applied as emitters in highly efficient solution-processed OLEDs to achieve EQE up to 14.3%. In 2020, Zhu *et al.* constructed an AIE dinuclear platinum(III) complex (**Pt103**, Fig. 13D) with a donor–acceptor type bridging ancillary ligand.[19] They proposed and validated the phosphorescence emission mechanism of the dinuclear platinum(III) complex, breaking the conventional non-emissive behavior of platinum(III) complexes. This breakthrough enabled the realization of room-temperature phosphorescence from platinum(III) complexes. **Pt103** was successfully applied in OLEDs, producing highly efficient organic electroluminescent devices with different emission colors (red to near-infrared). This study expanded the application of platinum(III) complexes in the field of OLEDs. Among them, the non-doped near-infrared device exhibited an emission wavelength of 716 nm, gaining a maximum EQE of 5.1%.[19]

In the field of organic optoelectronics, platinum complexes are primarily utilized for their high luminescence efficiency, high exciton utilization efficiency, and stable molecular structure. The AIE properties of platinum complexes effectively suppress the ACQ effect, making them a viable choice for constructing non-doped, high-efficiency optoelectronic devices.

4.3 Stimuli responses

Organic materials with multi-stimulus response (MSR) hold great potential in the field of optoelectronics, including applications such as optical data recording,[97] security labeling,[98] chemical sensors,[99–102] biomedical devices,[103,104] and OLEDs.[105] The MSR characteristics are mainly associated with molecular structural transitions, phase changes, excited-state transitions, chemical structures, and synergistic effects.[106] Platinum(II) complexes possess unique molecular structures and a variety of electronic transition types, thereby endowing them with multi-stimulus response properties.[74,107,108]

In 2016, Laskar *et al.* reported a platinum(II) complex (**Pt115**) with MSR properties, such as solvatochromic, mechanochromic, and AIE properties.[107] **Pt115** exhibited significant friction-induced color change during grinding, transitioning from yellow to orange emission. By crushing **Pt115** with mesoporous silica, a luminescent composite material was formed, and the luminescence color changed from yellow to green upon **Pt115** entering the mesoporous silica (Fig. 14A). The author proposed that after grinding, the molecules transformed from a crystalline to an amorphous state, and due to the proximity of the molecules under external forces, significant Pt–Pt interactions occurred, leading to a noticeable red-shift in luminescence. When **Pt115** was ground with silica, **Pt115** gradually adsorbed onto the silica, disrupting the dimeric structure of the molecules, and thus resulting in emission from monomers.

In 2020, Moreno *et al.* reported a cyclometalated platinum(II) complex (**Pt53**) based on an alkyne and isocyanide auxiliary ligand, which showed obvious solvatochromic, mechanochromic, vapochromic, and AIE properties (Fig. 14B).[74] After grinding, **Pt53** changed from a pale yellow to a deep yellow color, accompanied by a shift in emission from yellow to orange. Upon adding a few drops of dichloromethane to the ground sample, the orange emission rapidly reverted to yellow. It suggested that grinding led to a decrease in the crystallinity of the powder sample, resulting in the transition from a crystalline to an amorphous state and from an ordered to a disordered structure, thus causing an emission red shift. Treating the amorphous powder with a few drops of dichloromethane restored the peak portions in the XRD spectrum. These multi-stimulus responsive molecules hold significant application value in data recording, security labeling, and chemical sensing.[74]

In 2019, Lodeiro *et al.* reported a cyclometalated platinum(II) complex with an asymmetric bis-pyrazole structure (**Pt116**). Due to the presence of long alkyl chains within the molecule and strong self-assembly capability in the solid state, **Pt116** exhibited liquid crystallinity and multi-stimuli-responsive properties at low temperatures. The columnar stacking was formed through Pt–Pt interactions between molecules. The luminescent behavior of **Pt116** could be controlled by manipulating the properties of molecular assemblies, such as temperature, pressure, vapor, or solvent presence (Fig. 14C).[108] Firstly, the authors conducted temperature-dependent experiments to

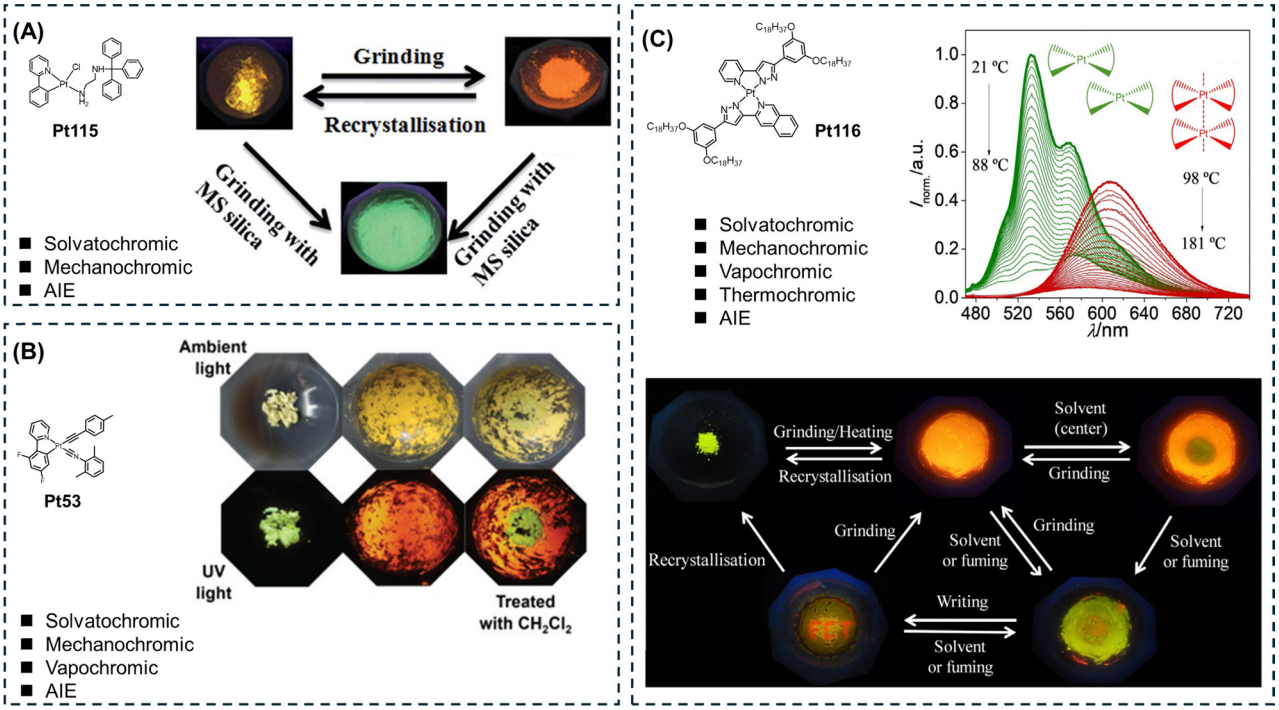

Fig. 14 Molecular structures and the multi-stimulus response performance of (A) **Pt115**, (B) **Pt53**, and (C) **Pt116**. Reprinted with permission from (A) ref. 107, (B) ref. 74, and (C) ref. 108. Copyright 2016 Royal Society of Chemistry, 2020 Royal Society of Chemistry, and 2019 Wiley-VCH, respectively.

analyze the luminescent and self-assembly behaviors of **Pt116**. Upon heating **Pt116**, the emission intensity gradually decreased due to thermally activated non-radiative processes. It should be noted that as the temperature approached the molecular melting point, the self-assembly of molecules *via* Pt–Pt interactions occurred, resulting in the appearance of a ^{3}MMLCT emission. As expected, further heating led to the quenching of the orange emission at around 180 °C. Building on the thermochromic behavior exhibited by **Pt116**, the authors further investigated the influence of external stimuli such as pressure/friction and vapor on the photophysical properties. In Fig. 14C, the initial emission of solid **Pt116** was observed as a green light. Grinding caused a rapid color change from green to orange within a few seconds, accompanied by an increase in PLQY from 2% to 20%. This phenomenon was attributed to the formation of aggregates in the solid state, leading to the existence of the ^{3}MMLCT excited state. For **Pt116**, solvent evaporation resulted in molecular self-assembly and the formation of an orange-emission thin film. Interestingly, the polarity of the solvent played a crucial role in the reversibility of the self-assembly behavior. By adding non-polar solvents such as hexane, toluene, tetrahydrofuran, dichloromethane, or chloroform, the monomeric binding mode of the compound could be restored, thereby recovering its initial green emission. Therefore, **Pt116** held huge potential for applications as a writable-readable-erasable material.[108]

4.4 Sensors and detectors

Cyclometalated platinum complexes, due to intermolecular interactions such as Pt–Pt interactions, exhibit a tendency to self-aggregate in the solid state, forming linear chains or oligomeric structures, which further induce changes in the absorption and/or emission of the system. The luminescent properties of these molecular species are highly dependent on the system's temperature, the type of counterions, and the solution concentration. By exploiting the photophysical changes during the aggregation and disaggregation processes of the molecules, cyclometalated platinum complexes have been widely applied in the fields of detection and sensing.[20,21] It has been found that polyelectrolytes such as single-stranded nucleic acids can cause significant changes in the UV-visible absorption and emission spectra of tridentate cyclometalated platinum(II) complexes.[62] The electrostatic binding between the positively charged cyclometalated platinum(II) complexes and the negatively charged single-stranded nucleic acids leads to an increase in the local concentration of the complexes, thereby inducing self-assembly of the cyclometalated platinum(II) complexes. The pronounced color changes and the emergence of new near-infrared emission bands are attributed to the formation of aggregates, which result in Pt–Pt interactions and/or π–π stacking, leading to MMLCT transitions.[20,21,42,61–63]

In 2017, Yam *et al.* introduced a water-soluble anionic tridentate cyclometalated platinum(II) complex (**Pt44**, Fig. 15A).[42] It undergoes supramolecular self-assembly with peptide segments enriched with cationic alanine through unique noncovalent Pt–Pt and π–π stacking interactions. When pancreatic trypsin is added, the alanine-enriched peptide segments can be hydrolyzed into smaller fragments, resulting in the disassembly of **Pt44**. The emission studies of the aggregated or disaggregated systems are conducted to explore the

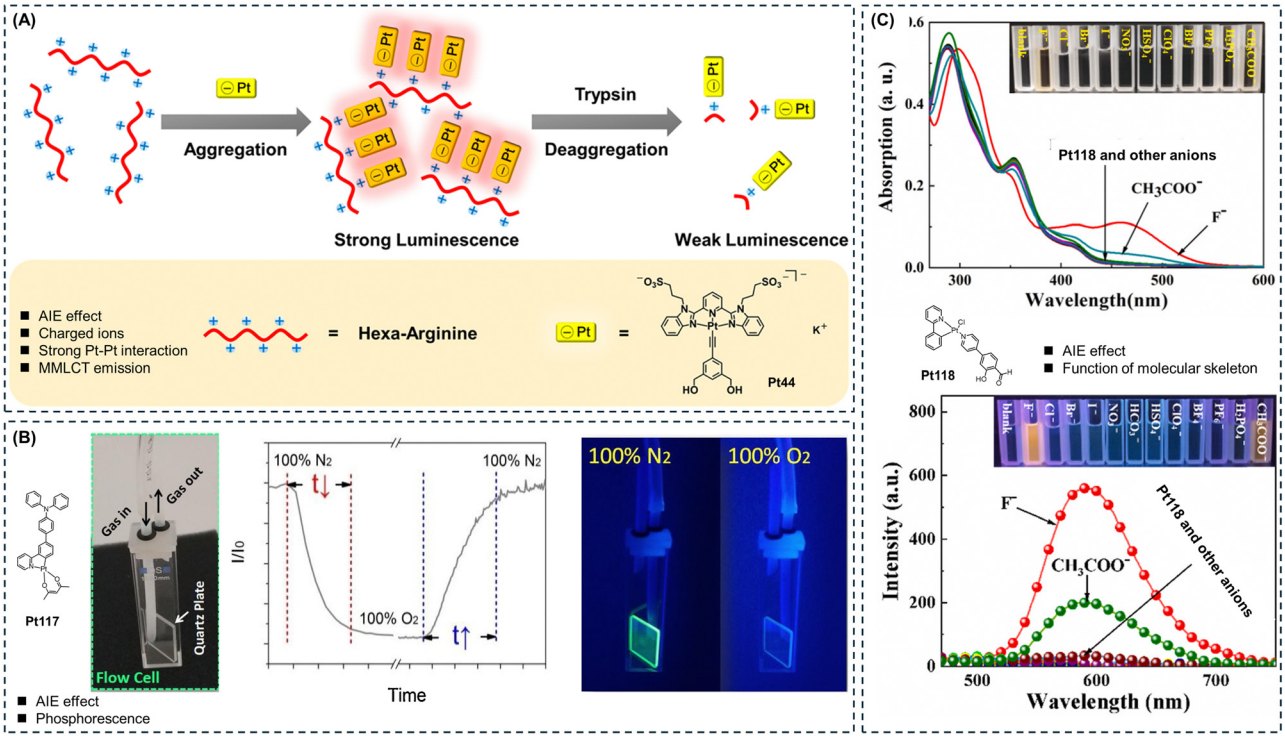

Fig. 15 (A) A schematic diagram depicting the design rationale for a continuous and label-free luminescence assay targeting trypsin is presented, utilizing an ensemble consisting of anionic **Pt44** and hexa-arginine. Reprinted with permission from ref. 42. Copyright 2017 American Chemical Society. (B) Oxygen sensing flow cell based on **Pt117**, the response time ($t\downarrow$) and recovery time ($t\uparrow$) of an oxygen-sensing film, and the photographs of the **Pt117**-EC(N10) film taken under 100% N_2 and 100% O_2. Reprinted with permission from ref. 60. Copyright 2021 Elsevier Ltd. (C) Changes of UV-vis absorption and emission change of **Pt118** in the presence of 3 equiv. of various anions in THF. Reprinted with permission from ref. 27. Copyright 2023 Elsevier Ltd.

aggregation–disaggregation process. **Pt44** is employed as a means to establish a novel method for continuous and label-free luminescent detection of trypsin, enabling both trypsin detection in diluted serum solutions and inhibitor screening with success.

In addition to utilizing the aggregation–disaggregation process of cyclometalated platinum(II) complexes for detecting specific compounds, in 2021, Yang *et al.* ingeniously employed the phosphorescent properties of cyclometalated platinum(II) complex **Pt117** to construct a luminescent oxygen sensing film in combination with low-cost ethyl cellulose (EC) (Fig. 15B).[60] Continuous monitoring of molecular oxygen with a luminescent oxygen sensor requires rapid quenching/recovery cycles and a short response time ($t\downarrow$) and recovery time ($t\uparrow$). Due to oxygen adsorption in the matrix, a delay is typically observed when the optical signal recovers to approximately 95% of its original state (100% N_2). $t\downarrow$. Due$t\uparrow$ accurately represent the time taken for the optical signal to extinguish and recover to 95%, respectively (Fig. 15B). Fig. 15B shows the luminescence images of the **Pt117**-EC(N10) film under 100% N_2 and 100% O_2, which can be accurately distinguished by the naked eye. The decrease in the thickness of the EC(N10) film exhibits a trend of reducing response and recovery time, achieving rapid quenching/recovery cycles within 7.7 seconds. AIE platinum(II) complexes greatly enhance the sensitivity and uniformity of the oxygen sensor.[60]

In 2023, Zhao *et al.* reported an AIE cyclometalated platinum(II) complex **Pt118** for the detection of fluoride ions.[27] The authors exquisitely utilized the acidity of the salicylic acid moieties in the complex for the specific detection of fluoride ions. The response behavior between **Pt118** and fluoride ions was studied through UV-visible absorption and photoluminescence spectroscopy. As shown in Fig. 15C, among various anions added, only F^- and CH_3COO^- caused significant UV-visible spectral changes, resulting in a new absorption band centered at around 460 nm and a visible color change from colorless to yellowish solution, which was visually observable. The blank solution showed no significant emission, but by adding various anions, only F^- and CH_3COO^- emitted bright orange luminescence with a peak around 596 nm. In comparison, the emission change caused by F^- ions was more obvious and faster than that by CH_3COO^- ions, while the addition of other ions hardly caused any emission change (Fig. 15C). These results manifested that **Pt118** may exhibit a more competitive emission response behavior towards F^- ions compared to CH_3COO^- ions and other ions, which could act as a luminescent sensor for highly sensitive detection of F^- ions.

The structural diversity of platinum complexes endows them with rich photoelectric properties and biological activities. Therefore, AIE platinum complexes are extensively employed in many fields, involving biological imaging and

therapy,[38–40,67,83] optoelectronics,[33–36] stimuli responses, sensing,[106–108] and detection.[61–63] In the biological field, current work on platinum compounds with four-ligand and six-ligand molecular frameworks has elaborately combined the imaging advantages of AIE molecules and the drug activity of cisplatin to achieve integrated diagnosis and treatment of cancer cells and tissues.[38–41] In the field of optoelectronics, especially OLEDs, platinum complexes with one-ligand, two-ligand, and three-ligand frameworks are widely applied as emitters in OLEDs due to their excellent stability and luminescent properties. Polynuclear platinum complexes are an advantageous strategy for constructing near-infrared-OLEDs due to their efficient ^{3}MMLCT or ^{3}LMMCT emission. Tridentate platinum complexes with a two-ligand framework have shone in the field of sensing and detection due to their excellent self-assembly properties.

5. Conclusions

AIE platinum complexes have been extensively applied in various fields due to their diverse structures and unique photophysical properties. This review that summarizes the AIE platinum complexes is of great significance as it helps to clarify the relationship between their molecular structures, photophysical properties, and applications. In general, AIE platinum complexes exhibit a wide range of molecular types, allowing for easy modulation of molecular structures and photophysical properties. This enables molecular design tailored to different applications. In the future development of AIE platinum complexes, the following points should be considered.

(1) There is still a large room for the development of AIE platinum complexes compared to AIE fluorescent materials. So far, there has been a lack of systematic research in this field, and the design and synthesis of AIE platinum complexes with specific functions are challenging. Therefore, future research should focus on studying the effects of the ligand structure and the number of ligands on their molecular optoelectronic properties and biological activities. This will broaden their applications in biomedical diagnosis and therapy, optoelectronic devices, multi-stimuli responsive systems, and sensing and detection.[109,110]

(2) The research on the AIE mechanism of platinum complexes lags behind that of AIE fluorescent molecules. Most of the studies on the AIE mechanism of platinum complexes have been based on the knowledge gained from AIE fluorescent molecules, such as using the AIE perturbation strategy. In the future, more in-depth research is needed on the AIE mechanism of AIE platinum complexes or other metal complexes. For example, can the AIE behavior of ligands be transferred to the complexes through AIE perturbation strategies?[111] What is the role of platinum ions in the AIE behavior of complexes? In this regard, the AIE platinum complexes with bidentate ligands have provided good answers to these questions. In such complexes, the self-assembly behavior of molecules induces Pt–Pt interactions, which in turn leads to the absorption and emission of MMLCT transition. However, other types of complexes have not been systematically studied. Therefore, a research paradigm can be considered, where the AIE behavior of the main ligands is compared with that of platinum complexes to further elucidate the role of metal ions in the AIE mechanism.

(3) During the study on the physicochemical properties of AIE platinum complexes, careful consideration should be given to the effects of aggregate environments, solvent systems, concentration, and changes in stimulus-responsive conditions on the properties of the molecules. This aspect of influence is often overlooked and its impact can be significant. The in-depth and meticulous studies on the effects of environmental changes on the luminescent properties of molecules are crucial for understanding the AIE mechanism.

(4) The expansion of the applications of AIE platinum complexes are vital, such as electrocatalysts.[112,113] On the one hand, the phosphorescence properties of platinum complexes can be exploited to extend their applications. Traditional fluorescent AIE molecules are abundant and it is thus essential to highlight the advantages of AIE phosphorescent materials or achieve functional complementarity with AIE fluorescent molecules. Recognizing the difference between AIE fluorescence and phosphorescence can greatly enhance the application value of the materials themselves. Therefore, leveraging the distinguishing properties of AIE platinum complexes, such as longer phosphorescence lifetime, larger absorption and emission wavelengths, and greater Stokes shift, is key to expanding the value of AIE phosphorescent materials. On the other hand, exploring the potential value of platinum ions is another important direction for expanding the applications of AIE platinum complexes. For example, in the field of bioimaging and therapeutics, the development of AIE platinum complexes will undoubtedly drive further advancements in platinum-based drugs.

(5) The research on polynuclear platinum complexes needs further advancement. First, how to obtain polynuclear platinum complexes in high yields is the first problem that needs to be solved. Second, how to exploit the inherent long-wavelength absorption or emission of polynuclear platinum complexes to further expand their applications? Then, polynuclear platinum complexes generally have large molecular weights and poor solubility, which largely limit their applications in biological, electronic, and other fields. Therefore, the subsequent research should focus on solving their solubility problem. At the same time, the AIE mechanism of polynuclear platinum complexes needs further in-depth study. Comparing the differences in the photophysical properties of mononuclear platinum complexes and polynuclear platinum complexes in the aggregate state is an important way to further understand the AIE mechanism. Finally, the construction of polynuclear multi-metal complexes is also a very interesting and challenging topic.[114] In addition, platinum metallacycles, platinum metallacages, and platinum-containing metal–organic frameworks should definitely be further developed in the future.

(6) In the study of ''aggregation-induced emission'', the previous work mainly focuses on ''induced emission'', *i.e.*,

exploring the phenomena of ''emission turn-on'' of specific systems and the reasons behind them. It is also quite important to explore the reasons for molecular aggregation and aggregation methods. How to describe and quantify the degree of aggregation of the system is an important issue that needs to be solved urgently. Therefore, future work needs to further develop the scientific connotation of aggregates, expand the means and characterization methods for studying the aggregate properties of molecules, and promote the innovation of aggregate research paradigms.

Conflicts of interest

There are no conflicts to declare.

Acknowledgements

This work was financially supported by the National Natural Science Foundation of China (21788102), the Research Grants Council of Hong Kong (16306620, 16307020, and C6014-20W), the Innovation and Technology Commission (ITC-CNERC14SC01, and ITCPD/17-9), Shenzhen Key Laboratory of Functional Aggregate Materials (ZDSYS20211021111400001), and the Science Technology Innovation Commission of Shenzhen Municipality (KQTD20210811090142053 and JCYJ20220818103007014).

References

1 J. Luo, Z. Xie, J. W. Y. Lam, L. Cheng, H. Chen, C. Qiu, H. S. Kwok, X. Zhan, Y. Liu, D. Zhu and B. Z. Tang, *Chem. Commun.*, 2001, 1740–1741.
2 J. Mei, N. L. C. Leung, R. T. K. Kwok, J. W. Y. Lam and B. Z. Tang, *Chem. Rev.*, 2015, **115**, 11718–11940.
3 H. Li, B. Jin, Y. Wang, B. Deng, D. Wang and B. Z. Tang, *Adv. Mater.*, 2023, **35**, 2210085.
4 Y. Duo, Y. Yang, T. Xu, R. Zhou, R. Wang, G. Luo and B. Zhong Tang, *Coord. Chem. Rev.*, 2023, **482**, 215070.
5 Y. Tu, Z. Zhao, J. W. Y. Lam and B. Z. Tang, *Natl. Sci. Rev.*, 2021, **8**, nwaa260.
6 V. Sathish, A. Ramdass, P. Thanasekaran, K.-L. Lu and S. Rajagopal, *J. Photochem. Photobiol., C*, 2015, **23**, 25–44.
7 L. Ravotto and P. Ceroni, *Coord. Chem. Rev.*, 2017, **346**, 62–76.
8 P. Alam, C. Climent, P. Alemany and I. R. Laskar, *J. Photochem. Photobiol., C*, 2019, **41**, 100317.
9 B. Manimaran, P. Thanasekaran, T. Rajendran, R.-J. Lin, I. J. Chang, G.-H. Lee, S.-M. Peng, S. Rajagopal and K.-L. Lu, *Inorg. Chem.*, 2002, **41**, 5323–5325.
10 V. W.-W. Yam, K. M.-C. Wong and N. Zhu, *J. Am. Chem. Soc.*, 2002, **124**, 6506–6507.
11 Q. Zhao, L. Li, F. Li, M. Yu, Z. Liu, T. Yi and C. Huang, *Chem. Commun.*, 2008, 685–687.
12 P. Thanasekaran, C.-C. Lee and K.-L. Lu, *Acc. Chem. Res.*, 2012, **45**, 1403–1418.
13 Z. Luo, X. Yuan, Y. Yu, Q. Zhang, D. T. Leong, J. Y. Lee and J. Xie, *J. Am. Chem. Soc.*, 2012, **134**, 16662–16670.
14 M. Yang, Y. Zhang, W. Zhu, H. Wang, J. Huang, L. Cheng, H. Zhou, J. Wu and Y. Tian, *J. Mater. Chem. C*, 2015, **3**, 1994–2002.
15 G. Li, R. S. Nobuyasu, B. Zhang, Y. Geng, B. Yao, Z. Xie, D. Zhu, G. Shan, W. Che, L. Yan, Z. Su, F. B. Dias and M. R. Bryce, *Chem. – Eur. J.*, 2017, **23**, 11761–11766.
16 H.-H. Zhang, J. Jing, G. Xu, Y.-X. Song, S.-X. Wu, X.-H. Chen, D.-S. Zhang, X.-P. Zhang and Z.-F. Shi, *Heliyon*, 2022, **8**, e11358.
17 W. Tao, Y. Chen, L. Lu and C. Liu, *Tetrahedron Lett.*, 2021, **66**, 152802.
18 J. Zhao, Z. Feng, D. Zhong, X. Yang, Y. Wu, G. Zhou and Z. Wu, *Chem. Mater.*, 2018, **30**, 929–946.
19 X. Wu, D.-G. Chen, D. Liu, S.-H. Liu, S.-W. Shen, C.-I. Wu, G. Xie, J. Zhou, Z.-X. Huang, C.-Y. Huang, S.-J. Su, W. Zhu and P.-T. Chou, *J. Am. Chem. Soc.*, 2020, **142**, 7469–7479.
20 V. W.-W. Yam, *Nat. Synth.*, 2023, **2**, 94–100.
21 M. H.-Y. Chan and V. W.-W. Yam, *J. Am. Chem. Soc.*, 2022, **144**, 22805–22825.
22 N. Komiya, T. Muraoka, M. Iida, M. Miyanaga, K. Takahashi and T. Naota, *J. Am. Chem. Soc.*, 2011, **133**, 16054–16061.
23 Y. Hu, K. H.-Y. Chan, C. Y.-S. Chung and V. W.-W. Yam, *Dalton Trans.*, 2011, **40**, 12228–12234.
24 S. Liu, H. Sun, Y. Ma, S. Ye, X. Liu, X. Zhou, X. Mou, L. Wang, Q. Zhao and W. Huang, *J. Mater. Chem.*, 2012, **22**, 22167–22173.
25 S. Lin, H. Pan, L. Li, R. Liao, S. Yu, Q. Zhao, H. Sun and W. Huang, *J. Mater. Chem. C*, 2019, **7**, 7893–7899.
26 X. Chen, Y. Sun, X. Zhao, X. Deng, X. Yang, Y. Sun, G. Zhou and Z. Wu, *Mater. Chem. Front.*, 2021, **5**, 4160–4173.
27 C. Li, L. Xu, J. A. Li, X. Chen, Z. Chi, B. Xu and J. Zhao, *Dyes Pigm.*, 2023, **209**, 110912.
28 Y. Sun, C. Zhu, S. Liu, W. Wang, X. Chen, G. Zhou, X. Yang and W.-Y. Wong, *Chem. Eng. J.*, 2022, **449**, 137457.
29 H. Yang, H. Li, L. Yue, X. Chen, D. Song, X. Yang, Y. Sun, G. Zhou and Z. Wu, *J. Mater. Chem. C*, 2021, **9**, 2334–2349.
30 J. Wu, B. Xu, Y. Xu, L. Yue, J. Chen, G. Xie and J. Zhao, *Inorg. Chem.*, 2023, **62**, 19142–19152.
31 N. H.-T. Le, R. Inoue, S. Kawamorita, N. Komiya and T. Naota, *Inorg. Chem.*, 2019, **58**, 9076–9084.
32 Z.-L. Gong, K. Tang and Y.-W. Zhong, *Inorg. Chem.*, 2021, **60**, 6607–6615.
33 Y.-C. Wei, K.-H. Kuo, Y. Chi and P.-T. Chou, *Acc. Chem. Res.*, 2023, **56**, 689–699.
34 K. Tuong Ly, R.-W. Chen-Cheng, H.-W. Lin, Y.-J. Shiau, S.-H. Liu, P.-T. Chou, C.-S. Tsao, Y.-C. Huang and Y. Chi, *Nat. Photonics*, 2017, **11**, 63–68.
35 Y.-C. Wei, S. F. Wang, Y. Hu, L.-S. Liao, D.-G. Chen, K.-H. Chang, C.-W. Wang, S.-H. Liu, W.-H. Chan, J.-L. Liao, W.-Y. Hung, T.-H. Wang, P.-T. Chen, H.-F. Hsu, Y. Chi and P.-T. Chou, *Nat. Photonics*, 2020, **14**, 570–577.
36 S.-F. Wang, B.-K. Su, X.-Q. Wang, Y.-C. Wei, K.-H. Kuo, C.-H. Wang, S.-H. Liu, L.-S. Liao, W.-Y. Hung, L.-W. Fu,

W.-T. Chuang, M. Qin, X. Lu, C. You, Y. Chi and P.-T. Chou, *Nat. Photonics*, 2022, **16**, 843–850.
37 J. Song, H. Xiao, L. Fang, L. Qu, X. Zhou, Z.-X. Xu, C. Yang and H. Xiang, *J. Am. Chem. Soc.*, 2022, **144**, 2233–2244.
38 Y. Yuan, R. T. K. Kwok, B. Z. Tang and B. Liu, *J. Am. Chem. Soc.*, 2014, **136**, 2546–2554.
39 Y. Yuan, Y. Chen, B. Z. Tang and B. Liu, *Chem. Commun.*, 2014, **50**, 3868–3870.
40 Y. Yuan, C.-J. Zhang and B. Liu, *Chem. Commun.*, 2015, **51**, 8626–8629.
41 B. Guo, M. Wu, Q. Shi, T. Dai, S. Xu, J. Jiang and B. Liu, *Chem. Mater.*, 2020, **32**, 4681–4691.
42 A. S.-Y. Law, M. C.-L. Yeung and V. W.-W. Yam, *ACS Appl. Mater. Interfaces*, 2017, **9**, 41143–41150.
43 A. S.-Y. Law, L. C.-C. Lee, M. C.-L. Yeung, K. K.-W. Lo and V. W.-W. Yam, *J. Am. Chem. Soc.*, 2019, **141**, 18570–18577.
44 H. Xiang, J. Cheng, X. Ma, X. Zhou and J. J. Chruma, *Chem. Soc. Rev.*, 2013, **42**, 6128–6185.
45 J. Zhang, F. Zhao, X. Zhu, W.-K. Wong, D. Ma and W.-Y. Wong, *J. Mater. Chem.*, 2012, **22**, 16448–16457.
46 C. Li, Y. Pang, Y. Xu, M. Lu, L. Tu, Q. Li, A. Sharma, Z. Guo, X. Li and Y. Sun, *Chem. Soc. Rev.*, 2023, **52**, 4392–4442.
47 S. Jamali, D. Milić, R. Kia, Z. Mazloomi and H. Abdolahi, *Dalton Trans.*, 2011, **40**, 9362–9365.
48 E. Nikoloudakis, I. López-Duarte, G. Charalambidis, K. Ladomenou, M. Ince and A. G. Coutsolelos, *Chem. Soc. Rev.*, 2022, **51**, 6965–7045.
49 R. C. Kwong, S. Sibley, T. Dubovoy, M. Baldo, S. R. Forrest and M. E. Thompson, *Chem. Mater.*, 1999, **11**, 3709–3713.
50 K. R. Graham, Y. Yang, J. R. Sommer, A. H. Shelton, K. S. Schanze, J. Xue and J. R. Reynolds, *Chem. Mater.*, 2011, **23**, 5305–5312.
51 S. J. Dorazio, A. Vogel, S. Dechert, D. E. Nevonen, V. N. Nemykin, C. Brückner and F. Meyer, *Inorg. Chem.*, 2020, **59**, 7290–7305.
52 C.-M. Che, S.-C. Chan, H.-F. Xiang, M. C. W. Chan, Y. Liu and Y. Wang, *Chem. Commun.*, 2004, 1484–1485.
53 M. Ikeshita, N. Hara, Y. Imai and T. Naota, *Inorg. Chem.*, 2023, **62**, 13964–13976.
54 J. Song, M. Wang, X. Zhou and H. Xiang, *Chem. – Eur. J.*, 2018, **24**, 7128–7132.
55 M. A. Soto, V. Carta, R. J. Andrews, M. T. Chaudhry and M. J. MacLachlan, *Angew. Chem., Int. Ed.*, 2020, **59**, 10348–10352.
56 A. I. Solomatina, E. E. Galenko, D. O. Kozina, A. A. Kalinichev, V. A. Baigildin, N. A. Prudovskaya, J. R. Shakirova, A. F. Khlebnikov, V. V. Porsev, R. A. Evarestov and S. P. Tunik, *Chem. – Eur. J.*, 2022, **28**, e202202207.
57 C. Cuerva, J. A. Campo, M. Cano, M. Caño-García, J. M. Otón and C. Lodeiro, *Dyes Pigm.*, 2020, **175**, 108098.
58 C. Cuerva, J. Fernández-Lodeiro, M. Cano, J. L. Capelo-Martínez and C. Lodeiro, *Nano Res.*, 2021, **14**, 245–254.
59 D. Tauchi, T. Koida, Y. Nojima, M. Hasegawa, Y. Mazaki, A. Inagaki, K.-I. Sugiura, Y. Nagaya, K. Tsubaki, T. Shiga, Y. Nagata and H. Nishikawa, *Chem. Commun.*, 2023, **59**, 4004–4007.
60 L. Di, Z. Xia, H. Wang, Y. Xing and Z. Yang, *Sens. Actuators, B*, 2021, **326**, 128987.
61 V. W.-W. Yam, K. H.-Y. Chan, K. M.-C. Wong and N. Zhu, *Chem. – Eur. J.*, 2005, **11**, 4535–4543.
62 C. Y.-S. Chung, K. H.-Y. Chan and V. W.-W. Yam, *Chem. Commun.*, 2011, **47**, 2000–2002.
63 C. Yu, K. H.-Y. Chan, K. M.-C. Wong and V. W.-W. Yam, *Chem. Commun.*, 2009, 3756–3758.
64 H.-K. Cheng, M. C.-L. Yeung and V. W.-W. Yam, *ACS Appl. Mater. Interfaces*, 2017, **9**, 36220–36228.
65 J. Wu, Y. Li, C. Tan, X. Wang, Y. Zhang, J. Song, J. Qu and W.-Y. Wong, *Chem. Commun.*, 2018, **54**, 11144–11147.
66 C. Po, A. Y.-Y. Tam, K. M.-C. Wong and V. W.-W. Yam, *J. Am. Chem. Soc.*, 2011, **133**, 12136–12143.
67 A. S.-Y. Law, L. C.-C. Lee, K. K.-W. Lo and V. W.-W. Yam, *J. Am. Chem. Soc.*, 2021, **143**, 5396–5405.
68 C. A. Strassert, C.-H. Chien, M. D. Galvez Lopez, D. Kourkoulos, D. Hertel, K. Meerholz and L. De Cola, *Angew. Chem., Int. Ed.*, 2011, **50**, 946–950.
69 N. K. Allampally, M. Bredol, C. A. Strassert and L. De Cola, *Chem. – Eur. J.*, 2014, **20**, 16863–16868.
70 A. Aliprandi, M. Mauro and L. De Cola, *Nat. Chem.*, 2016, **8**, 10–15.
71 S. Carrara, A. Aliprandi, C. F. Hogan and L. De Cola, *J. Am. Chem. Soc.*, 2017, **139**, 14605–14610.
72 X. Hao, B. Xiong, M. Ni, B. Tang, Y. Ma, H. Peng, X. Zhou, I. I. Smalyukh and X. Xie, *ACS Appl. Mater. Interfaces*, 2020, **12**, 53058–53066.
73 J. R. Berenguer, E. Lalinde, M. T. Moreno, S. Sánchez and J. Torroba, *Inorg. Chem.*, 2012, **51**, 11665–11679.
74 M. Martínez-Junquera, R. Lara, E. Lalinde and M. T. Moreno, *J. Mater. Chem. C*, 2020, **8**, 7221–7233.
75 H. Wang, Y. Yan, S. Gan, H. Tu, X. Jiang, S. Zhu, G. Song, R. Liu and H. Zhu, *Inorg. Chim. Acta*, 2023, **555**, 121578.
76 Y. Zhang, F. Meng, C. You, S. Yang, L. Xiong, W. Xiong, W. Zhu, Y. Wang, Y. Pei and S. Su, *Dyes Pigm.*, 2017, **142**, 457–464.
77 X. Yang, L. Yue, Y. Yu, B. Liu, J. Dang, Y. Sun, G. Zhou, Z. Wu and W.-Y. Wong, *Adv. Opt. Mater.*, 2020, **8**, 2000079.
78 Y. Li, D. P.-K. Tsang, C. K.-M. Chan, K. M.-C. Wong, M.-Y. Chan and V. W.-W. Yam, *Chem. – Eur. J.*, 2014, **20**, 13710–13715.
79 R. Liu, S. Zhu, J. Lu, H. Shi and H. Zhu, *Dyes Pigm.*, 2017, **147**, 291–299.
80 Y. Ai, Y. Li, H. L.-K. Fu, A. K.-W. Chan and V. W.-W. Yam, *Chem. – Eur. J.*, 2019, **25**, 5251–5258.
81 W. J. Mullin, H. Qin, T. Mani, P. Müller, M. J. Panzer and S. W. Thomas, *Chem. Commun.*, 2020, **56**, 6854–6857.
82 K. Peng, B.-B. Liang, W. Liu and Z.-W. Mao, *Coord. Chem. Rev.*, 2021, **449**, 214210.
83 Y. Gao, J. Zhang, Z. He, L. Luo and C. Yan, *Org. Electron.*, 2021, **92**, 106105; M.-X. Zhu, W. Lu, N. Zhu and C.-M. Che, *Chem. – Eur. J.*, 2008, **14**, 9736–9746.
84 M.-X. Zhu, W. Lu, N. Zhu and C.-M. Che, *Chem. – Eur. J.*, 2008, **14**, 9736–9746.

85 S. Yu-Lut Leung and V. Wing-Wah Yam, *Chem. Sci.*, 2013, **4**, 4228–4234.
86 B. Das and P. Gupta, *Dalton Trans.*, 2021, **50**, 10225–10236.
87 J. Song, M. Wang, X. Xu, L. Qu, X. Zhou and H. Xiang, *Dalton Trans.*, 2019, **48**, 4420–4428.
88 V. W.-W. Yam, K. H.-Y. Chan, K. M.-C. Wong and B. W.-K. Chu, *Angew. Chem., Int. Ed.*, 2006, **45**, 6169–6173.
89 H.-L. Au-Yeung, S. Y.-L. Leung and V. W.-W. Yam, *Chem. Commun.*, 2018, **54**, 4128–4131.
90 J. Chen, L. Ao, C. Wei, C. Wang and F. Wang, *Chem. Commun.*, 2019, **55**, 229–232.
91 L. Qu, C. Li, G. Shen, F. Gou, J. Song, M. Wang, X. Xu, X. Zhou and H. Xiang, *Mater. Chem. Front.*, 2019, **3**, 1199–1208.
92 J. Song, H. Xiao, B. Zhang, L. Qu, X. Zhou, P. Hu, Z.-X. Xu and H. Xiang, *Angew. Chem., Int. Ed.*, 2023, **62**, e202302011.
93 Y. Wang, J. Nie, W. Fang, L. Yang, Q. Hu, Z. Wang, J. Z. Sun and B. Z. Tang, *Chem. Rev.*, 2020, **120**, 4534–4577.
94 J. Wang, J. Li, L. Wang, T. Han, D. Wang and B. Z. Tang, *ACS Appl. Polym. Mater.*, 2020, **2**, 4306–4318.
95 B. Li, Y. Wang, M. H.-Y. Chan, M. Pan, Y. Li and V. W.-W. Yam, *Angew. Chem., Int. Ed.*, 2022, **61**, e202210703.
96 H. Yersin, *Highly efficient OLEDs with phosphorescent materials*, John Wiley & Sons, 2008.
97 Y. Liu, J. Duan, F. Qi, D. Tian, X. Wang, Z. Liu and W. Huang, *Dalton Trans.*, 2017, **46**, 10332–10338.
98 Y. Shen, X. Le, Y. Wu and T. Chen, *Chem. Soc. Rev.*, 2024, **53**, 606–623.
99 H. Zhu, J. Fan, B. Wang and X. Peng, *Chem. Soc. Rev.*, 2015, **44**, 4337–4366.
100 Z. Chi, X. Zhang, B. Xu, X. Zhou, C. Ma, Y. Zhang, S. Liu and J. Xu, *Chem. Soc. Rev.*, 2012, **41**, 3878–3896.
101 B. Xu, H. Wu, J. Chen, Z. Yang, Z. Yang, Y.-C. Wu, Y. Zhang, C. Jin, P.-Y. Lu, Z. Chi, S. Liu, J. Xu and M. Aldred, *Chem. Sci.*, 2017, **8**, 1909–1914.
102 Y. Liang, P. Hu, H. Zhang, Q. Yang, H. Wei, R. Chen, J. Yu, C. Liu, Y. Wang, S. Luo, G. Shi, Z. Chi and B. Xu, *Angew. Chem., Int. Ed.*, 2024, **63**, e202318516.
103 M. Zeng, D. Zavanelli, J. Chen, M. Saeidi-Javash, Y. Du, S. LeBlanc, G. J. Snyder and Y. Zhang, *Chem. Soc. Rev.*, 2022, **51**, 485–512.
104 M. Yang, Z. Zeng, J. W. Y. Lam, J. Fan, K. Pu and B. Z. Tang, *Chem. Soc. Rev.*, 2022, **51**, 8815–8831.
105 S.-Y. Yang, Y.-K. Qu, L.-S. Liao, Z.-Q. Jiang and S.-T. Lee, *Adv. Mater.*, 2022, **34**, 2104125.
106 Q. Liao, Q. Li and Z. Li, *Adv. Mater.*, 2023, **35**, 2306617.
107 S. S. Pasha, P. Alam, A. Sarmah, R. K. Roy and I. R. Laskar, *RSC Adv.*, 2016, **6**, 87791–87795.
108 C. Cuerva, J. A. Campo, M. Cano and C. Lodeiro, *Chem. – Eur. J.*, 2019, **25**, 12046–12051.
109 M. E. Gutierrez Suburu, M. Blanke, L. Geerkens, A. Hepp, I. Maisuls, J. Kösters, T. Neumann, J. Voskuhl, M. Giese and C. A. Strassert, *Aggregate*, 2024, **5**, e473.
110 Z.-L. Gong, Z.-Q. Li and Y.-W. Zhong, *Aggregate*, 2022, **3**, e177.
111 Z. Zhao, Z. Wang, J. Tavakoli, G. Shan, J. Zhang, C. Peng, Y. Xiong, X. Zhang, T. S. Cheung, Y. Tang, B. Huang, Z. Yu, J. W. Y. Lam and B. Z. Tang, *Aggregate*, 2021, **2**, e36.
112 N. D. Loewen, T. V. Neelakantan and L. A. Berben, *Acc. Chem. Res.*, 2017, **50**, 2362–2370.
113 C. Cesari, J.-H. Shon, S. Zacchini and L. A. Berben, *Chem. Soc. Rev.*, 2021, **50**, 9503–9539.
114 Y. Sun and P. J. Stang, *Aggregate*, 2021, **2**, e94.